CHDR

Centre for Human Drug Research

Analyzing psychophysical and electrophysiological data using mixed-effect models

Quantification of stimulus processing using intra-epidermal electrodes

Author:
Alexander Mentink, MSc

Examination committee:
Dr. ir. Robert-Jan Doll, CHDR
Prof. dr. Frans van der Helm, Delft University of Technology
Dr. ir. Jan Buitenweg, Twente University
Dr. ir. Jacob Söhl, Delft University of Technology
Dr. ir. Mark van de Ruit, Delft University of Technology

University, Master program & specialization:
Delft University of Technology
Biomedical Engineering
Biomechatronics

October 18, 2017

Contents

Abstract

Background: One of the biggest challenges of analyzing electroencephalogram (EEG) data in pain processing is the low signal-to-noise ratio (SNR). A common method to increase the SNR is to average time-locked responses over repeated trials. Unfortunately, relevant information is lost due to averaging. In addition, EEG responses are influenced by psychophysical elements, such as stimulus intensity and stimulus detection. Therefore, to reduce the loss of information and to control for psychophysical elements we developed a novel analysis method using linear mixed-effect (LME) models. Furthermore, capsaicin was used to challenge the novel method with the goal to quantify peripheral and central sensitization effects.

New method: LME models were used to include all EEG trials into one model to reduce the loss of information caused by averaging. In addition, phase locked and non-phase locked EEG data were combined with psychophysical data to control for psychophysical elements.

Results: Including all EEG trials into one model made it possible to perform statistical analyses. Moreover, combining EEG data with psychophysical data showed effects of stimulus detection, stimulus amplitude and the number of pulses on EEG responses. Although the LME models were able to test for significant effects after capsaicin application, the analyses did not show sensitization effects.

Comparison with existing methods: The phase locked EEG data was analyzed using conventional time-domain averaging methods and compared with LME models which included all EEG trials into one model.

Conclusion: This study showed that the novel LME method could be used to perform statistical analyses using all EEG trials and detect significant differences over time. In addition, psychophysical elements such as stimulus detection, amplitude and number of pulses could be controlled for both phase locked and non-phase locked EEG analyses. Probably, attention and learning effects played a role in the interpretation of the effects of capsaicin. Although application of this novel method showed no peripheral and central sensitization effects induced by capsaicin, it did show the potential of LME models in phase locked and non-phase locked EEG analyses.

Introduction

Since pain is the most common reason to visit a doctor [1, 2, 3] and because many pain problem remain unrelieved [4], it is necessary to improve the treatment of pain. This may be done by creating a more thorough understanding of pain processing which allows for targeting analgesics more effectively. Understanding mechanisms underlying pain can be done by using a known input to stimulate the pain system and subsequently recording the related output. In other words, to quantify responses evoked by well-controlled noxious stimuli. Information on the relationships between stimulus and response in combination with knowledge on physiological pathways may give more insight into pain related processes.

Transcutaneous electrical stimulation using surface electrodes is a common method to evoke pain in an experimental setting [5, 6]. However, this method activates both $A\beta$-fibers and $A\delta$-fibers. Since $A\beta$-fibers are primarily responsible for sensory signals and $A\delta$-fibers transmit the 'pinprick-like' pain signals, it is important to reduce the co-activation of $A\beta$-fibers to be able to quantify specific mechanisms related to the pain system. Recent studies showed that intra-epidermal electrical stimulation (IES) proved to be a well-controlled noxious stimulation technique that preferentially stimulates $A\delta$-fibers [7, 8, 9]. IES uses electrodes with small needles that are inserted into the epidermis. The needles in combination with relatively low currents activate nociceptive $A\delta$-fibers while minimizing the co-activation of non-nociceptive $A\beta$-fibers [10, 8]. Quantification of the related responses to IES can be done by both psychophysical methods and electrophysiological methods.

An important psychophysical method is based on fitting the stimulus amplitudes and correlated responses (e.g. detected/not-detected) to a psychophysical function[1]. The psychophysical function describes the stimulus detection probability given the stimulus intensity using a sigmoidal relationship (Fig 1) [11]. The parameters that can be extracted from this psychophysical function are the detection threshold (α), i.e. stimulus amplitude at 0.5 detection probability, and the slope (β), i.e. the steepness of the curve. Since these parameters are sensitive to changing stimulus properties [12, 13, 14, 15] or interventions [16], they can be used as quantifiers of pain processing. Furthermore, psychophysical methods can be used to find facilitatory pain mechanisms by relating detection thresholds of a theoretical double pulse with an observed double pulse [17]. According to probability summation, the detection probability of a double pulse is dependent on the detection probability of each individual pulse (p_s) [18]. Assuming that both pulses in a double pulse stimulus are independent (i.e. equal detection probability), the detection probability of a theoretical double pulse (p_d) can be estimated by pure probability summation: $p_d = (1-p_s)^2$. Therefore, the psychophysical curve of a double pulse could be estimated by using the psychophysical curve of a single pulse. Differences between the theoretical double pulse and the observed double pulse may give information on underlying facilitatory pain mechanisms.
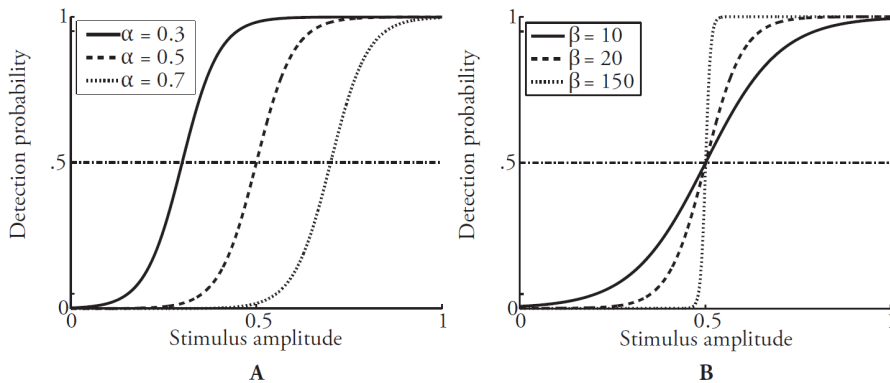

*Figure 1: Example of a psychophysical function relating the stimulus amplitude to the detection probability. **A)** A shift in the detection threshold (α) results in a horizontal displacement of the psychophysical curve. **B)** A shift in slope (β) results in a change in steepness of the psychophysical curve. Illustration from Doll et al. [19]*

---

[1]More information on psychophysical analyses can be found in the Appendix II: Psychophysical data analysis.

The most commonly used electrophysiological method for the quantification of pain processing is electroencephalography (EEG). EEG data concerning pain related processes can be analyzed by phase locked and non-phase locked analyses. The assumption of phase locked analyses is that the phase of each oscillatory response is the same, while non-phase locked analyses also take into account temporal dispersion of oscillatory responses[2]. In case of phase locked analyses, the response typically consists of a biphasic negative (N) – positive (P) wave corrected for baseline, i.e. evoked potential (EP). The most common parameters that are extracted from these EPs are peak amplitudes and latencies. The amplitude mainly depends on the habituation of the receptor and the intensity & the salience of the stimulus. The latency of the peak mainly depends on the type of fiber that is stimulated, the signal processing time and the location on the body where it is stimulated [20]. Non-phase locked analyses are based on estimating the amplitude or power of oscillations as a function of time and frequency. The oscillatory power of prespecified regions of interest (ROIs) in a time-frequency representation (TFR) can be used as an estimate of pain-related processes [21, 22].

One of the biggest challenges of analyzing EEG data concerning pain related processes is the low signal-to-noise ratio (SNR). Some of the noise can be reduced easily by removing unnecessary electromagnetic sources from the experimental setting or removing contaminated EEG trials (due to muscle contractions or ocular movements). However, some of the internal background noise that is present in a living brain cannot be removed easily. A commonly used technique to increase the SNR is averaging of time-locked responses over repeated trials (e.g. Fig 2). This technique is based on the assumption that the background noise is uncorrelated and that the responses are always comprised of signals with comparable characteristics. The useful peak parameters that are related to pain processing can be extracted after averaging. Subsequently, these parameters can be used as endpoints in a statistical model (e.g. ANOVA) to find significant differences between measurements.

Unfortunately, recent studies indicate that the background noise is not completely uncorrelated due to asymmetric amplitude fluctuations [23, 24]. In addition, electrophysiological responses are influenced by psychophysical elements, such as stimulus intensity and stimulus detection [25]. Moreover, across-trial variability of electrophysiological responses may contain relevant information that is lost by averaging over repeated trials. Especially when the number of trials per measurement are limited or the stimulus intensity is low, averaging may be insufficient to extract relevant parameters. Subsequently, this will affect ordinary statistical analyses and result in wrong conclusions.
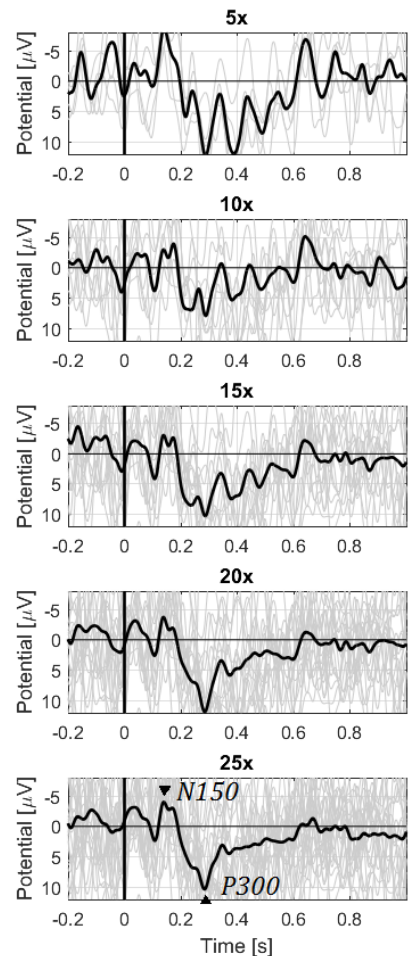

Figure 2: The effect of averaging of single trial evoked responses on the signal-to-noise ratio. Note that at least 20 single trials without artifacts are needed to extract useful parameters related to pain processing, i.e. peak amplitudes and latencies around 150 and 300 ms.

---

[2]For more information on temporal dispersion and non-phase locked information loss, see Appendix IV: Non-phase locked analyses

A novel technique to analyze EEG data to reduce the loss of information caused by averaging is the use of linear mixed-effect models (LME models). These models describe the relationship between a response variable and independent variables using fixed and random effects. The fixed effects describe the linear regression part, while the random effects are used to assign the causes of interindividual variability with a predefined distribution. In a more practical sense, LME models in EEG analyses may be used to describe the relationship between the amplitude or power of the electrophysiological signal to independent variables such as time, location of stimulation or intervention, while taking into account the between-subject variability.

LME models for phase locked EEG data can describe the amplitude of an EP over time. This means that for each time point in the EEG trial, a single LME model is created that describes the EP amplitude at that time point (Fig 3a). LME models for non-phase locked EEG data can describe the power within a TFR. A specified region can be selected for each trial and information may be extracted that can be used as a response variable in a LME model (Fig 3b). Importantly, both types of LME models can be used to combine the EEG data with psychophysical data to control for the effect of the stimulus intensity or the effect of a detected/not-detected stimulus on the electrophysiological response.

(a) Phase locked analysis
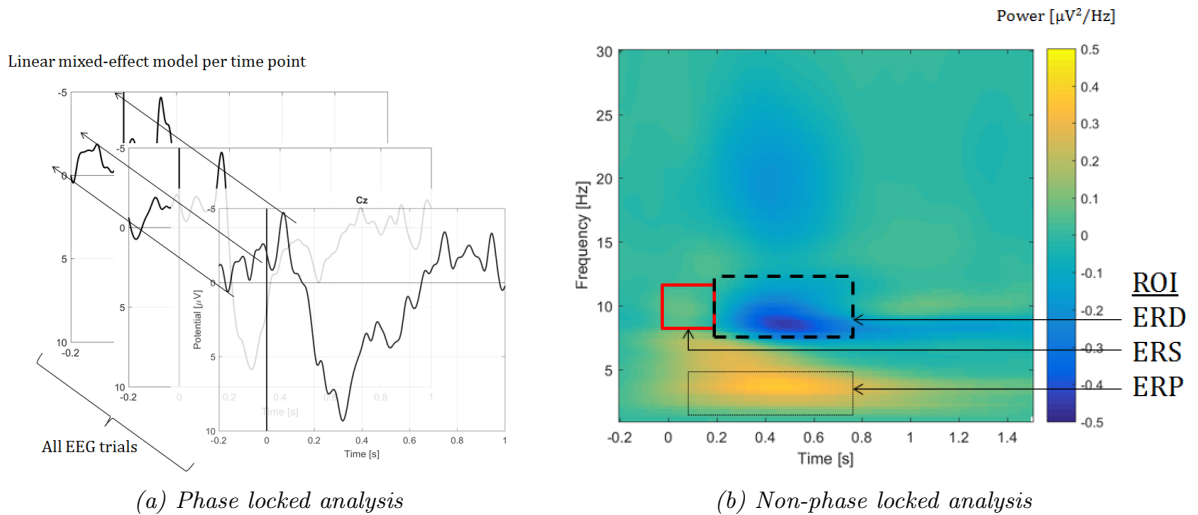
(b) Non-phase locked analysis

*Figure 3: EEG data can be analyzed by phase locked and non-phase locked techniques. **a)** Three single EEG trials are shown to illustrate the concept of linear mixed-effect modeling on phase locked evoked potentials (EPs). Ordinary time-domain averaging (Fig 2) loses information about across-trial variability. Using linear mixed-effect models to estimate the EP amplitude takes into account all EEG trials and can be combined with the related psychophysical data. **b)** Time-frequency representation (TFR) after IES. Interpretation of TFRs is based on the transient increase, i.e. event related synchronization (ERS), or decrease, i.e. event related desynchronization (ERD), of power in a specific frequency band. Prominent EPs are ERSs that can be found primarily at the central midline lead (Cz) with a frequency between 2-4 Hz [26]. Other ERSs may be found in the alpha frequency band (8-12 Hz) and are thought to play a role in cortical deactivation or inhibition, while ERDs in the same band are thought to resemble cortical activation or disinhibition [27]. In this report, the event-related potentials (ERPs) are the EPs including latency-jitter.*

Here we introduce the novel analysis method of phase locked and non-phase locked EEG data combined with psychophysical data using LME models. This method is applied in combination with a pain modulation compound, i.e. capsaicin. Capsaicin is a highly selective agonist for the vanniloid receptor 1 (TRPV1), which is an important transducer of noxious thermal and chemical evoked stimulations [28]. The activation of TRPV1 may result in peripheral and central sensitization effects. Peripheral sensitization effects cause a reduction in pain threshold on the site of application, i.e. primary area, and central sensitization effects cause a reduction in pain threshold on the site surrounding the application, i.e. secondary area[3].

---

[3]For a more elaborate explanation see Appendix I: Neuropathic pain and capsaicin model

In this study, quantification of peripheral and central sensitization are done by stimulating the primary and secondary areas using IES and analyzing the psychophysical and EEG responses. Psychophysical analyses are performed by modeling the stimuli and correlated responses to a psychophysical function to extract detection thresholds and slopes. In addition, EEG analyses are performed by time-domain averaging and linear mixed-effect models. Importantly, two novel EEG analyses are introduced. First, LME models per time point are used to combine the psychophysical with phase locked electrophysiological data including all EEG trials. Second, LME models are used to combine psychophysical data with non-phase locked power values of predefined TF-ROIs including all EEG trials.

Problem statement and goal
Since the common method of averaging of EEG data results in loss of information and ignores psychophysical effects, a novel EEG analysis method is introduced in this paper. The first goal is to optimize EEG analyses by including all trials in a LME model and to control for psychophysical elements. Subsequently, the second goal is to apply this novel EEG analysis method by quantifying peripheral and central sensitization effects induced by capsaicin.

Methods

Subjects

Experiments were performed on 21 healthy male subjects (18-45y). The study was approved by the medical ethics review board in Assen (Beoordeling Ethiek Biomedisch Onderzoek). In accordance with the Declaration of Helsinki, written informed consent was given by the subjects before participation in the study. Subjects were to have a body mass index between 18-30 kg/m^2 (inclusive) and were in good medical condition according to their medical history, physical examination and vital signs. All subjects were able to refrain from strenuous physical exercise 48 hours prior to admission and prior to each stay at the clinic. Exclusion criteria were dark skin (Fitzpatrick scale type V or VI), illicit drug use, frequent caffeine use (>8 units/day), smokers (>10 cigarettes/day), extreme responders to topical capsaicin 1% cream (NRS >8/10), skin abnormalities and abnormal blood pressure. No over-the-counter medication within 3 days of nociceptive measurements could be used. Subjects unable to refrain from smoking or consuming coffee during each stay at the CHDR were excluded. Subjects unable to tolerate the assessments at screening were excluded. The subjects each received remuneration for participating in the study and could withdraw at anytime without jeopardising this remuneration.

Study design

The study was set up as an open-label, parallel-group study. A total of 21 subjects attended the clinic during the screening and on 2 occasions, each with a wash-out period of 7 days. One subject got sick halfway the first occasion and was therefore excluded from all analyses. This paper is part of a larger study conducting several pharmacodynamic assessments. Capsaicin application, safety and pharmacodynamic assessments were performed at time points specified in the Appendix V: Schedule of Assessments. The pharmacodynamic assessements related to this paper are depicted in Fig 4. The IES and EEG measurements were done before capsaicin application (baseline) and twice after capsaicin application (+1h & +8h). The thermode was used to confirm the effect op capsaicin by quantification of heat pain detection thresholds[4].

Assessments	Scr	Base	-30m	0	+20m	+1h	+3h	+5h	+8h	+10h
Capsaicin	▬		▬▬▬							
IES + EEG		▬				▬			▬	
Thermode	▬	▬			▬	▬	▬	▬	▬	▬

Figure 4: Schedule of pharmacodynamic assessments for one occasion. IES was performed in three stimulation blocks: at baseline, after 1h and 8h of capsaicin application. Scr = screening, Base = baseline, IES = intra-epidermal electrical stimulation, EEG = electroencephelogram.

Capsaicin application

Preparation

Prior to application, three different areas were marked using a template: primary, secondary and control. The site of application was called the primary area and was a 3x3 cm square on the right volar forearm, approximately 10 cm distal from the elbow pit. The secondary area was an octogonal area 2 cm outside of the primary area. The control area was the same as the primary area, but on the contralateral side, i.e. the left volar forearm.

Capsaicin

Topical cream consisting of 1% capsaicin was manufactured and validated by the pharmacy of the Leiden University Medical Center. The cream was applied on the primary area and covered by a cotton gaze. After 30 min the capsaicin was wiped off with clean gaze and ethanol[5].

---

[4]The results of the thermode are shown in the Appendix VI: Results primary heat hyperalgesia.

[5]For more extensive information on the capsaicin application methods see Appendix VIII: Standard Operating Protocols.

Intra-epidermal electrical stimulation

Stimulator and electrodes

The stimulator that was used for IES was the Ambustim (NociTRACK B.V.). The stimulation electrode was a non-invasive concentric bipolar needle electrode consisting of 5 anodic needles. The cathode was a self-adhesive transcutaneous electrical nerve stimulation (TENS) electrode that was placed distal from the stimulation electrode. The stimuli were constant-current rectangular single and double pulses with a pulse width of 420 μs, inter-pulse interval of 10 ms and a randomized inter-stimulus interval of 2.5-3.5 s.

Experimental procedure

The subject was asked to press the response button to start the experiment, release the button briefly when a stimulus was felt and repress the button to continue the experiment. The stimulus pattern generation and the recording of the responses was done by LabVIEW 2013, National Instruments. The recording of the EEG was done by TMSi Polybench software.

Each IES stimulation block was divided into stimulation of three consecutive areas, 1) Secondary, 2) Primary, 3) Control, lasting 15 min each. EEG was recorded during the entire stimulation block and trigger pulses were used to identify the stimulus types and amplitudes, thereby allowing the combination of psychophysical data with electrophysiological data. The stimulus selection procedure was based on Monte Carlo simulations[6].
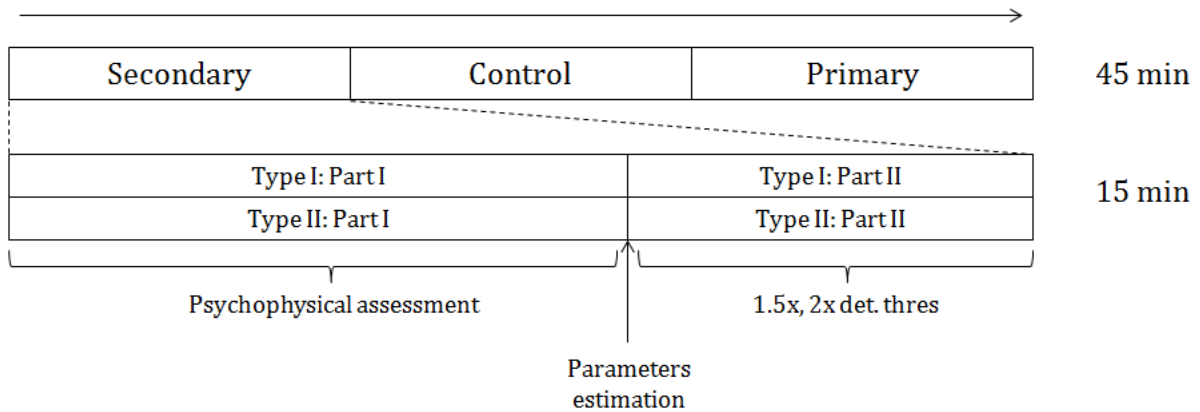

Figure 5: *Overview of one stimulation block of intra-epidermal electrical stimulation. The secondary and primary areas were the expected secondary and primary hyperalgesia areas on the right volar forearm. The control area was on the contralateral side of the primary area, i.e. the left volar forearm. The stimulation of each area was divided into two parts. Part I consisted of the psychophysical curve estimation in which the detection threshold and the slope was estimated real-time. Subsequently, Part II consisted of stimulating 20 times at 1.5x and 2x the detection threshold. Within Part I and II, two stimulation types were distinguished: single pulses (Type I) and double pulses (Type II).*

Psychophysical analyses

The psychophysical data were analyzed using MATLAB 2016b, Mathworks. The detection probability p for detecting a stimulus of amplitude x [mA] was modeled with a logistic psychophysical function:

$$p(x; \alpha(t), \beta) = \left(1 + e^{\beta(\alpha(t) - x)}\right)^{-1} \tag{1}$$

where $\alpha(t)$ and β were the detection threshold and slope parameter of the psychophysical function, respectively[7]. This relationship was fitted using a two step generalized linear model-linear mixed-effect

---

[6]For more information on the stimulus selection procedure, see the Appendix III: Stimulus selection procedure
[7]For more information on the psychophysical analyses see Appendix II: Psychophysical data analysis

model (GLM-LME model). First, the response variables α (detection threshold) and β (slope) were estimated for each measurement over time using GLM with a logit link function (Eq 1). Subsequently, both response variables were placed in two linear mixed-effect models using the following relationship:

$$y = X\beta + Zb + \epsilon \qquad (2)$$

For which:
- y is the n-by-1 response vector, with n observations/trials
- X is an n-by-p fixed-effects design matrix, with p variables related to fixed effects
- β is an p-by-1 fixed-effects vector
- Z is an n-by-q random-effects design matrix, with q variables related to random effects
- b is a q-by-1 random-effects vector
- ϵ is a n-by-1 observation error vector

Eq was used to model two response variables, i.e. the detection probability (α) and the slope (β). In addition, these LME models were used for two reasons. First, to find an effect of the stimulus type on the psychophysical parameters using baseline data only. Second, to find an effect of the capsaicin on the psychophysical parameters. Therefore, the following models were translated into MATLAB using 'fitlme'.

$\alpha \sim \underbrace{\texttt{Time+Type}}_{\text{Fixed effects}}+\underbrace{\texttt{(1+Area|Subject)}}_{\text{Random effects}}$ [8]

$\beta \sim \underbrace{\texttt{Time+Type}}_{\text{Fixed effects}}+\underbrace{\texttt{(1+Area|Subject)}}_{\text{Random effects}}$ [9]

$\alpha \sim \underbrace{\texttt{Time+Area*Measurement*Type}}_{\text{Fixed effects}}+\underbrace{\texttt{(1+Area+Measurement|Subject)}}_{\text{Random effects}}$ [10]

$\beta \sim \underbrace{\texttt{Time+Area*Measurement*Type}}_{\text{Fixed effects}}+\underbrace{\texttt{(1+Area+Measurement|Subject)}}_{\text{Random effects}}$ [11]

The independent variables were both continuous and categorical. `Time` (0-420 s) was a continuous variable and the other independent variables were categorical. `Area` was related to the Control, Primary and Secondary hyperalgesia areas. `Measurement` was either Baseline (pre-dose), +1 hour or +8 hours after capsaicin removal. `Type` was related to the single or double pulse stimulus and `Subject` was related to subject number S1-S20. Post-hoc contrast analyses were performed on the fixed effects to study differences in detection thresholds and slopes.

EEG recording

The EEG data were recorded using a 40-channel Refa system by TMSI (Twente Medical Systems International B.V.; sampling rate, 1024 Hz) using a 24-channel EEG cap based on the extended 10-20 system. All channels were kept below 5 kΩ impedance and were grounded at AFz. artefacts caused by eye blinks and ocular movements were recorded using two surface electrodes; one placed on the right side of the lower right eyelid and one place on the left side of the upper left eyelid. The central midline lead referenced to the mean of all channels (Cz-Avg) was used for all analyses.

---

[8] This LME model was used to show the effect of the stimulus type on the detection threshold using baseline data only.
[9] This LME model was used to show the effect of the stimulus type on the slope using baseline data only.
[10] This LME model was used to show the effect of the capsaicin on the detection threshold.
[11] This LME model was used to show the effect of the capsaicin on the slope.

EEG Analyses

The psychophysical data were analyzed using MATLAB 2016b, Mathworks in combination with the FieldTrip Toolbox [29].

Preprocessing

EEG data were preprocessed using FieldTrip, an open-source toolbox running under the MATLAB environment. First, the trials were configured using 1s prestimulus and 1s poststimulus time interval. Subsequently, the psychophysical stimulus-response-time (SRT) data were loaded and triggers from the EEG and SRT were used to align the datasets. The EEG data was bandpass filtered at 0.5-30 Hz and baseline corrected using the 500-0 ms prestimulus interval. Trials containing eye blink artefacts were removed using automatic rejection of trials containing potentials larger than 4 times the standard deviation based on either the EOG or Fpz channel.

Phase locked analyses

Time-domain averaging
Grand averages were weighted by the number of trials and averaged over the time-domain averages of individual results of all areas per measurement. Individual plots were visually inspected and distinguishable peaks were extracted. Two examples were selected to show the quality of the results. No statistical analyses could be performed using time-domain averaging.

Linear mixed-effect model
Linear mixed-effect modeling was used to model the EP amplitude at each time point in the EEG trial. The original data was downsampled to 100 Hz. Since each trial was defined as 1s pre and 1s post stimulus, a total amount of 201 models were needed for each analysis. Eq was used to model one response variable, i.e. the EP amplitude per time point. These LME models were used for five reasons. First, to find an effect of the stimulus detection on the EP amplitude using baseline data only. Second, to find an effect of the stimulus amplitude on the EP amplitude using baseline data only. Third, to find an effect of the stimulus type at the same stimulus amplitude on the EP amplitude using baseline data only. Fourth, to find an effect of the stimulus amplitude at the same detection threshold on the EP amplitude using baseline data only. Fifth, to find an effect of the capsaicin on the EP amplitude. Therefore, the following models were translated into MATLAB using 'fitlme'.

$$EP \sim \underbrace{\texttt{Response }}_{\text{Fixed effects}} + \underbrace{\texttt{(1+Area|Subject)}}_{\text{Random effects}}{}^{12}$$

$$EP \sim \underbrace{\texttt{Response+Stim}}_{\text{Fixed effects}} + \underbrace{\texttt{(1+Area|Subject)}}_{\text{Random effects}}{}^{13}$$

$$EP \sim \underbrace{\texttt{Response+Stim*Type}}_{\text{Fixed effects}} + \underbrace{\texttt{(1+Area|Subject)}}_{\text{Random effects}}{}^{14}$$

$$EP \sim \underbrace{\texttt{Response+Thres*Type}}_{\text{Fixed effects}} + \underbrace{\texttt{(1+Area|Subject)}}_{\text{Random effects}}{}^{15}$$

$$EP \sim \underbrace{\texttt{Response+Stim*Area*Measurement*Type}}_{\text{Fixed effects}} + \underbrace{\texttt{(1+Area+Measurement|Subject)}}_{\text{Random effects}}{}^{16}$$

---

[12] This LME model was used to show the effect of the stimulus detection on the EP amplitude using baseline data only.

[13] This LME model was used to show the effect of the stimulus amplitude on the EP amplitude using baseline data only.

[14] This LME model was used to show the effect of the stimulus type at the same stimulus amplitude on the EP amplitude using baseline data only.

[15] This LME model was used to show the effect of the stimulus type at the same detection threshold on the EP amplitude using baseline data only.

[16] This LME model was used to show the effect of capsaicin on the EP amplitude using all data.

The response variable `EP` was the continuous evoked potential amplitude per time point in every trial. The independent variables were continuous and categorical. `Stim` was the absolute IES stimulus amplitude and the only continuous independent variable, `Thres` was a categorical measure related to the detection threshold per measurement classified as 0x, 1x, 1.5x and 2x detection threshold. `Response` was the stimulus detection, either detected or not detected. The other categorical variables are described in the previous paragraph. Post-hoc contrast analyses were performed on the fixed effects to study differences in amplitudes per time point.

Non-phase locked analyses

Time-frequency analyses
A Hanning window was used to estimate the time-frequency representations (TFR), for more information on the TFR and TF-ROIs see Fig 3b. The frequency of interest was 1-30 Hz using steps of 0.25 Hz, the time of interest was -3-2.5 s using steps of 10 ms and the number of cycles of the Hanning window was 7. All TFRs were baseline corrected using the 500-0 ms prestimulus interval. The time-frequency region of interests (TF-ROIs) were event-related desynchronizations (ERDs), event-related synchronizations (ERSs) and event-related potentials (ERPs). The TF-ROIs were based on suppressions and elevations in the grand averages[17] and were very comparable to literature [27, 30]. ROI-ERD was defined between 200-800 ms and 7-12 Hz, ROI-ERS was defined between 0-200 ms and 8-11 Hz and the ROI-ERP was defined between 100-800 ms and 2-4 Hz. For the ROI-ERD the lowest 20% values were selected and the mean was calculated. For the ROI-ERS and ROI-ERP the top 20% values were selected and the mean was calculated. This technique is used to avoid noise and is successfully used in other studies as well [22, 27]. The mean values of these top 20% and bottom 20% were used as response variables in the LME models.

Linear mixed-effect model
Linear mixed-effect modeling was used to model the TF-ROIs over all trials. These were translated into the following LME models using MATLAB's function fitlme:

$$\text{ERD} \sim \underbrace{\text{Response+Stim*Area*Measurement*Type+}}_{\text{Fixed effects}}\underbrace{\text{(1+Area+Measurement|Subject)}}_{\text{Random effects}}{}^{18}$$

$$\text{ERS} \sim \underbrace{\text{Response+Stim*Area*Measurement*Type+}}_{\text{Fixed effects}}\underbrace{\text{(1+Area+Measurement|Subject)}}_{\text{Random effects}}{}^{19}$$

$$\text{ERP} \sim \underbrace{\text{Response+Stim*Area*Measurement*Type+}}_{\text{Fixed effects}}\underbrace{\text{(1+Area+Measurement|Subject)}}_{\text{Random effects}}{}^{20}$$

The response variables `ERD`, `ERS`, `ERP` were continuous. The independent variables were the same continuous and categorical variables as the LME models for the phase-locked analyses. Post-hoc contrast analyses were performed on the fixed effects to show significant differences.

---

[17]For more information see Appendix: VII: Time-frequency representations - Grand averages
[18]This LME model was used to show the effect of the capsaicin on the ERD power values.
[19]This LME model was used to show the effect of the capsaicin on the ERS power values.
[20]This LME model was used to show the effect of the capsaicin on the ERP power values.

Results

Psychophysical

The psychophysical data consisted of stimulus amplitudes and responses (detected vs not-detected stimuli) over time, see Fig 6 for a typical data set. In total 360 data sets were recorded, consisting of 20 subjects, 2 occasions, 3 measurement blocks and 3 areas. All data sets were visually inspected and a data set was rejected when it was considered invalid. The reasons for this were wrongful executions or technical difficulties. In total 336 data sets were used for all the analyses. The plotted psychophysical curves were the estimated curves at 210 s (halfway Part I).
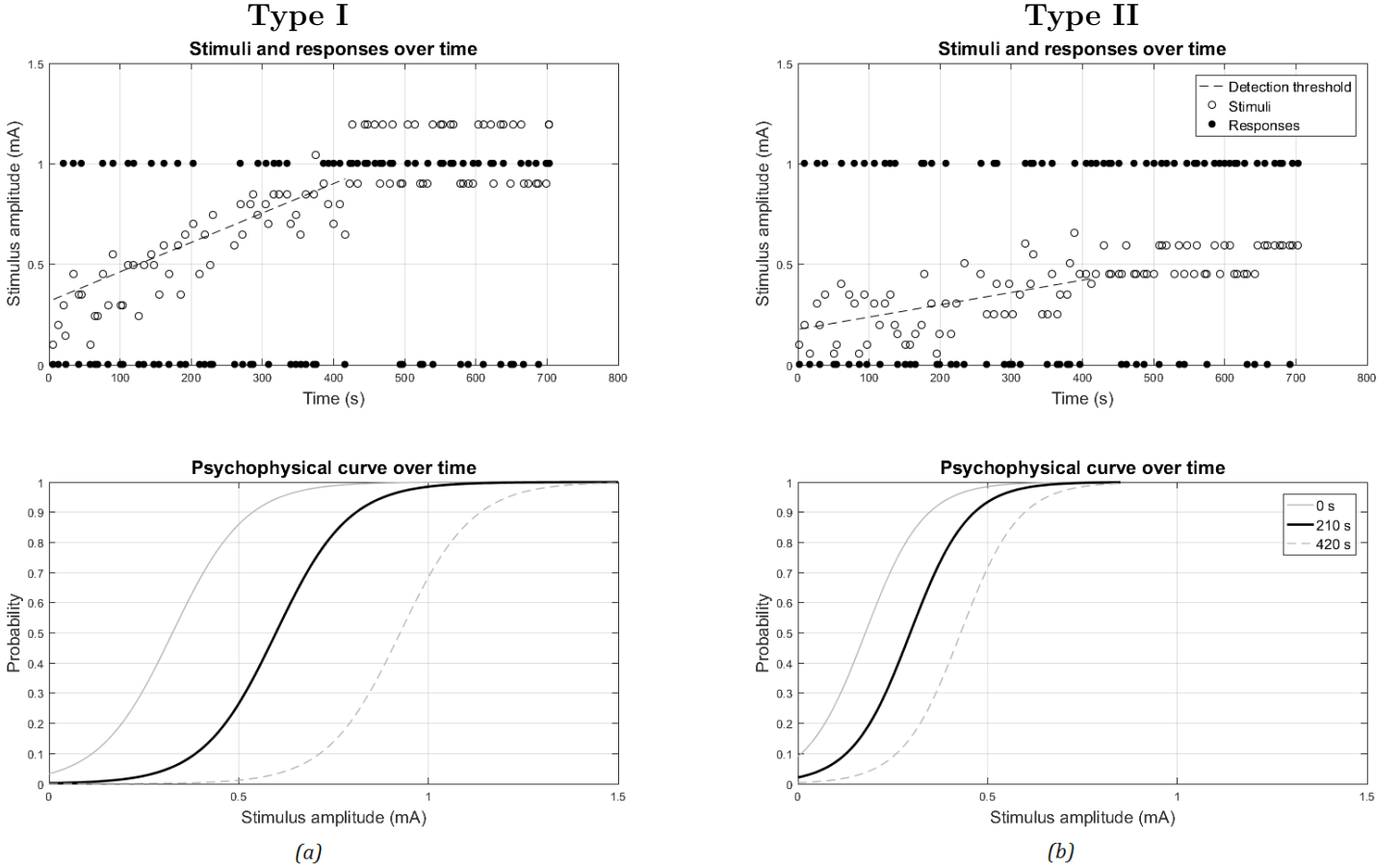

*Figure 6: Typical example of a psychophysical data set. The data set contained two stimulus types (single and double pulse) and consisted of two parts. Part I lasted 420 s and was used to estimate the psychophysical parameters over time. Part II was comprised of 2×20 stimulations at $1.5\times$ and $2\times$ detection threshold. The responses were either 0 (not-detected) or 1 (detected) and the amplitude range depicted the range in which stimulus amplitudes could be given according to the stimulus selection procedure. **a)** Top: Single pulse stimuli and responses with the estimated detection threshold over time. Bottom: Estimated psychophysical curve at 210 s with related parameters: $\alpha = 0.60$ mA and $\beta = 10.39$ mA^{-1}. **b)** Top: Double pulse stimuli and responses with the estimated detection threshold over time. Bottom: Estimated psychophysical curve at 210 s with related parameters: $\alpha = 0.30$ mA and $\beta = 13.00$ mA^{-1}.*

Effect of stimulus type on psychophysical curve

Figure 7 shows the effect of stimulus type (single or double pulse) on the psychophysical curve estimation using baseline measurements only. Double pulse stimulation shows significantly lower detection thresholds (0.30 mA) compared to single pulse stimulation (0.61 mA). In addition, double pulse stimulation shows significantly higher slopes (22.76 mA^{-1}) compared to single pulse stimulation (10.71 mA^{-1}). Moreover, facilitatory processes resulted in lower detection thresholds for the measured double pulse stimulation than the expected double pulse stimulation based on pure probability summation.
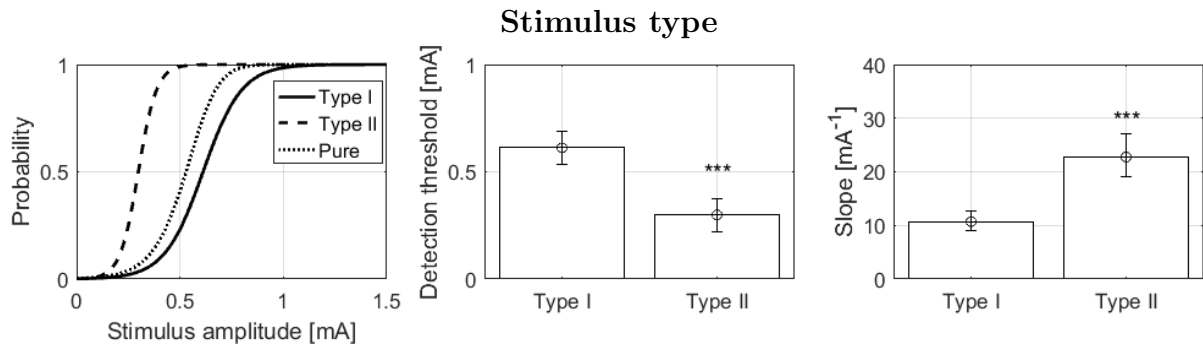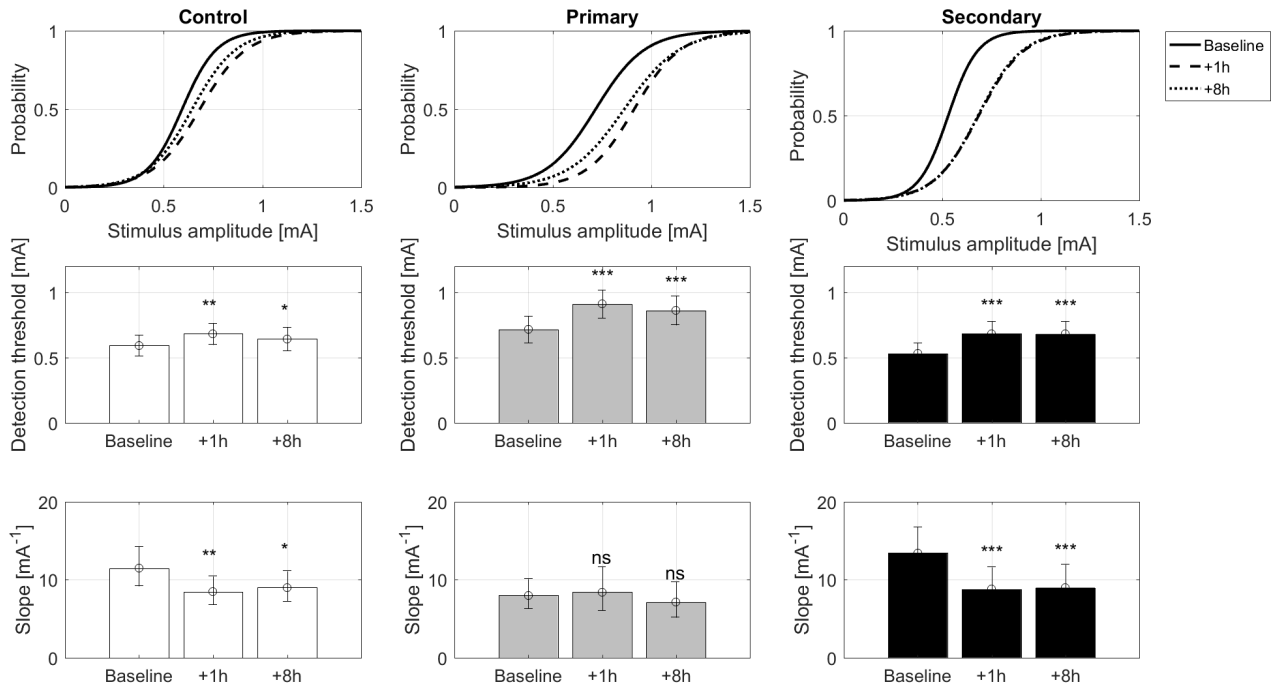
Figure 7: Psychophysical curves, related detection thresholds and slopes for single (Type I), double pulse (Type II) stimulation and pure probability summation for baseline measurements only. Notice the temporal summation effect of the observed double pulse compared with the expected double pulse (pure probability summation). Bars represent 95% confidence intervals. Significant differences between Type I vs Type II are depicted by asterisk (p≥.05=ns, p<.05=*, p<.01=**, p<.001=***)

Effect of capsaicin on psychophysical curve

Figure 8 shows the effect of capsaicin on the psychophysical curve estimation for both single (Type I) and double (Type II) pulse stimulation. Single pulse stimulation shows significant increases of detection thresholds after administration of capsaicin for all areas. Significant decreases in slope can be seen for the control and secondary areas. Type II shows significant increases of the detection threshold for both the primary and secondary areas. Significant decreases in slope can be seen for the control and secondary areas.
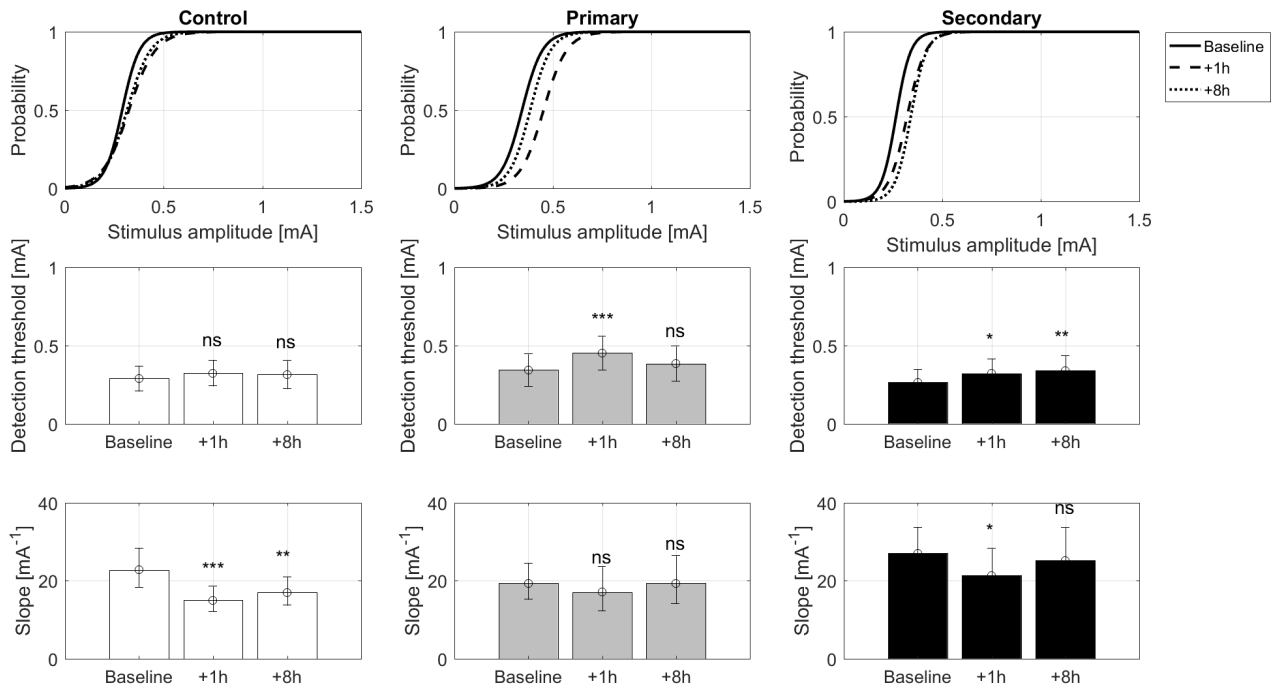
Type I

Type II

Figure 8: Psychophysical curves, related detection thresholds and slopes for single (Type I) and double pulse (Type II) stimulation per area per measurement. Bars represent 95% confidence intervals. Note the different axis scales for detection thresholds and slopes between Type I and II. Significant differences between +1h vs baseline and +8h vs baseline are depicted by asterisk (p≥.05=ns, p<.05=*, p<.01=**, p<.001=***)

EEG

Phase locked analyses

Time-domain averaging

All time-domain averaged EPs were visually inspected and about 14% of the data contained visually distinguishable N150 and P300 peaks. Therefore, no statistical analyses could be performed on the N150/P300 peak amplitudes or latencies to find significant differences between measurements or areas. To illustrate the quality of the time-domain averaged EPs, an example of a usable and unusable EP is shown in Fig 9. The grand averages per area per measurement are shown in Fig 10. This figure shows overall trends.
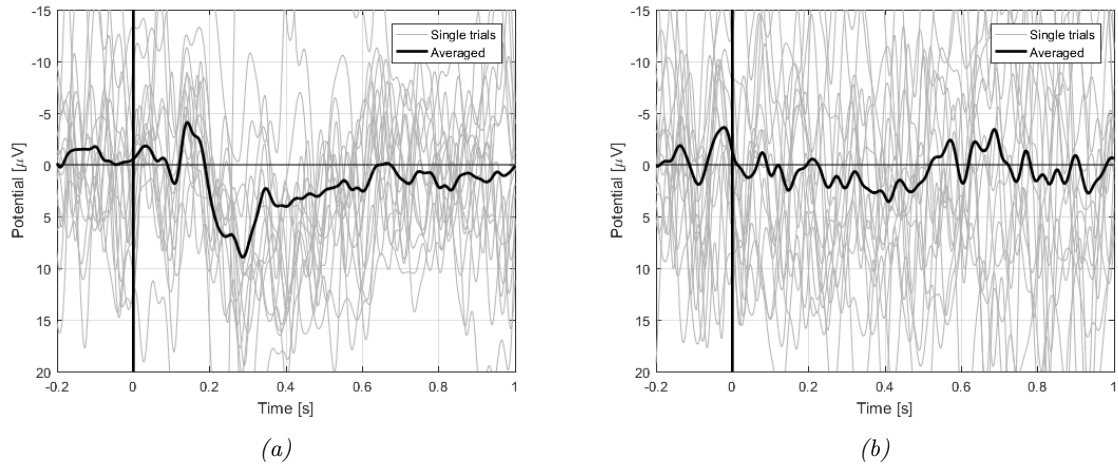

Figure 9: Typical examples of time-domain averaged evoked potentials (EPs) averaged using ±30 trials. These examples illustrate the quality of the EP data in this study, emphasizing the fact that no statistical analysis could be performed. **a)** *Example of an EP showing distinguishable peaks. These resemble approximately 14% of the data.* **b)** *Example of an EP showing no distinguishable peaks. These resemble approximately 86% of the data.*

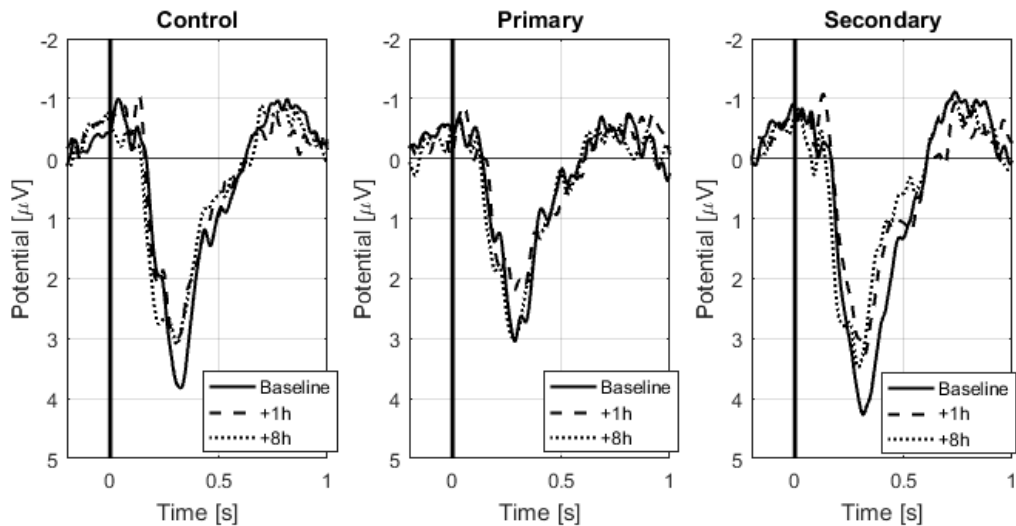*Figure 10: The grand averages of evoked potentials using time-domain averaging per area per measurement. Decreasing trends can be noticed in the absolute amplitudes of P300 over measurement per area and within each measurement block (Secondary - Control - Primary). Unfortunately, the peaks of individual time-domain averaged measurements contained too many indistinguishable components for statistical analysis.*

15

Effect of psychophysical data on EP amplitudes
Fig 11 shows the effect of psychophysical data on the EP amplitude using LME models. The most important effect is the stimulus detection, whether a stimulus is detected or not. Figure 11a shows that the P300 amplitude of a detected stimulus compared to a not-detected stimulus is significantly higher. In addition, the stimulus amplitude also has an effect on the EP amplitude, showing significant increases between 0.13-0.28 s (Fig 11b). The stimulus type shows elevated P300 amplitudes after double pulse compared to single pulse stimulation (Fig 11c), but is not affected when the EP is corrected for detection threshold (Fig 11d).

Effect of capsaicin on EP amplitudes
Figures 12 and 13 show the effect of capsaicin on the EPs for both single and double pulse stimulation at fixed stimulus amplitudes. The stimulus amplitudes were chosen close to 100% detection probability of the mean, i.e. 1.00 mA for a single pulse and 0.50 mA for a double pulse (see Fig 7). Single pulse stimulation shows significantly lower P300 amplitudes for stimulus amplitudes after administration of capsaicin at the control and secondary area. Note that baseline compared to +8h after administration shows largest and longest reductions. Double pulse stimulation shows significantly lower P300 amplitudes after administration of capsaicin at the secondary area mostly. In addition, P300 amplitudes are significantly lower at baseline for primary areas compared to secondary areas.

Non-phase locked analyses

Effect of capsaicin on TF-ROIs
Figures 14 and 15 show the effect of capsaicin on the ERD, ERS and ERP power values for both single and double pulse stimulation at fixed stimulus amplitudes. Single pulse stimulation shows no significant effects after administration of capsaicin. Double pulse stimulation shows significant increases in ERS power values after administration of capsaicin for the secondary area. In addition, increased trends of ERP power values after administration of capsaicin for the secondary area can be noticed as well.
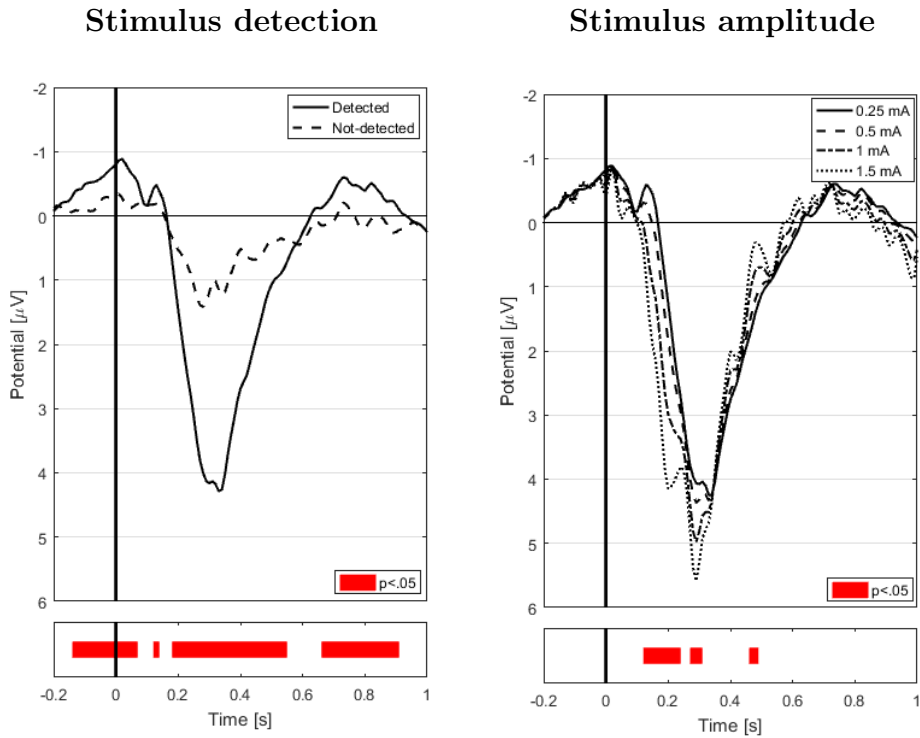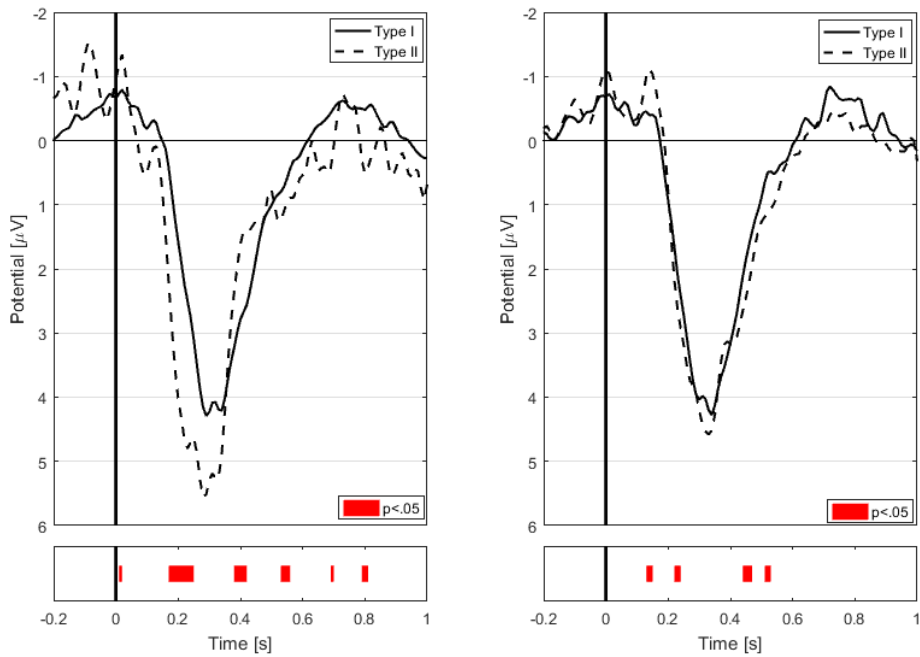
Figure 11: Combining psychophysical data with evoked potential amplitudes using linear mixed-effect models. **a)** Evoked potentials are influenced by stimulus detection. When a stimulus is detected, the P300 peak amplitude is increased for a time range of 0.18-0.55 s with a maximal increase of 3.01 mA. **b)** Evoked potentials are influenced by the stimulus amplitude. When the stimulus amplitude is increased, the P300 peak amplitude is increased for a time range of 0.12-0.31 s. Notice the latency shift. **c)** Evoked potentials are influenced by the stimulus type at the same stimulus amplitude. This plot shows evoked potentials that are detected and are stimulated at 0.50 mA. The P300 peak amplitude of a double pulse is increased for a time range of 0.17-0.25 s with a maximal increase of 1.40 mA compared to a single pulse. Notice the latency shift. **d)** Evoked potentials are minimally influenced by the stimulus type at 1x detection threshold (d.t.). The bars represents significant differences per time point (p<.05).
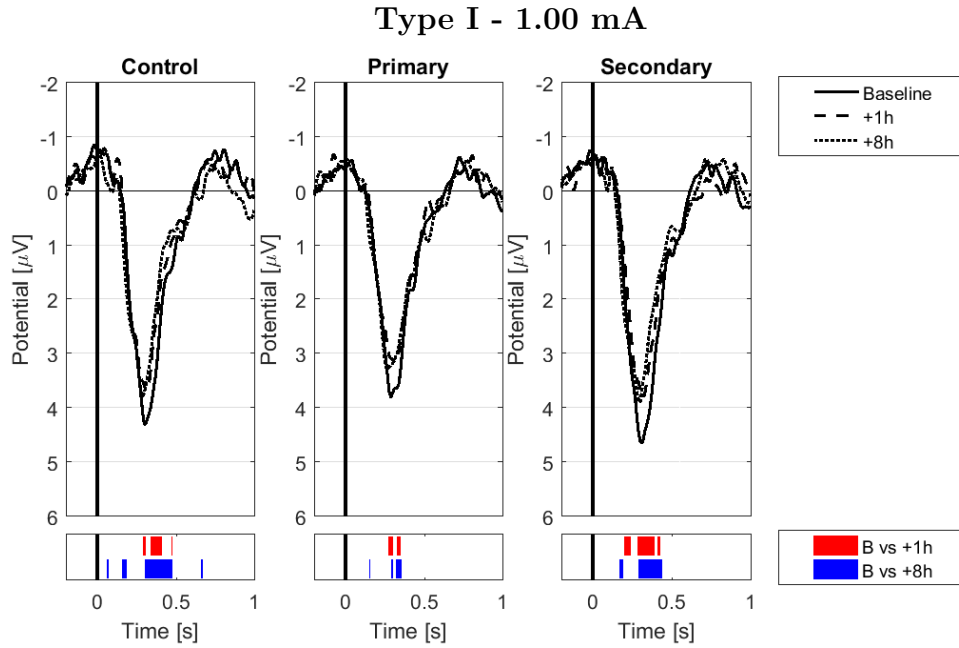
Figure 12: Evoked potentials for single pulse stimulation per area per measurement at a fixed stimulus amplitude of 1.00 mA (around twice the detection threshold). Post hoc analyses were performed to show the significant differences between baseline and +1h/+8h measurements within each area over time. This is visualized by the red and blue bars that represent significant differences per time point within each area (p<.05). Notice the significant larger P300 peak amplitudes at baseline for each area.

Figure 13: Evoked potentials for double pulse stimulation per area per measurement at a fixed stimulus amplitude of 0.50 mA (around twice the detection threshold). Post hoc analyses were performed to show the significant differences between baseline and +1h/+8h measurements within each area over time. This is visualized by the red and blue bars that represent significant differences per time point within each area (p<.05). Notice the significant larger P300 peak amplitudes at baseline for primarily the secondary area.
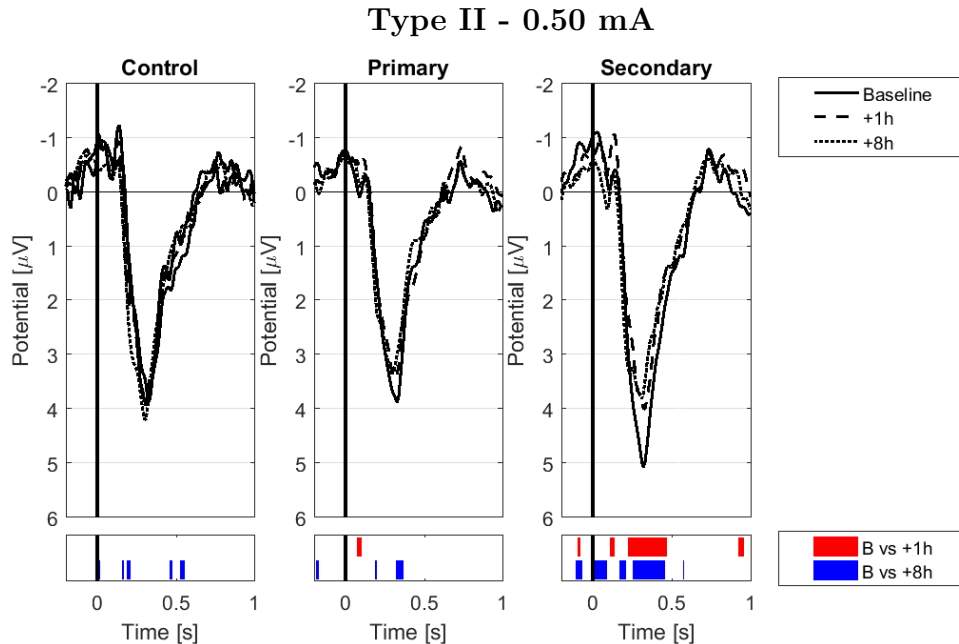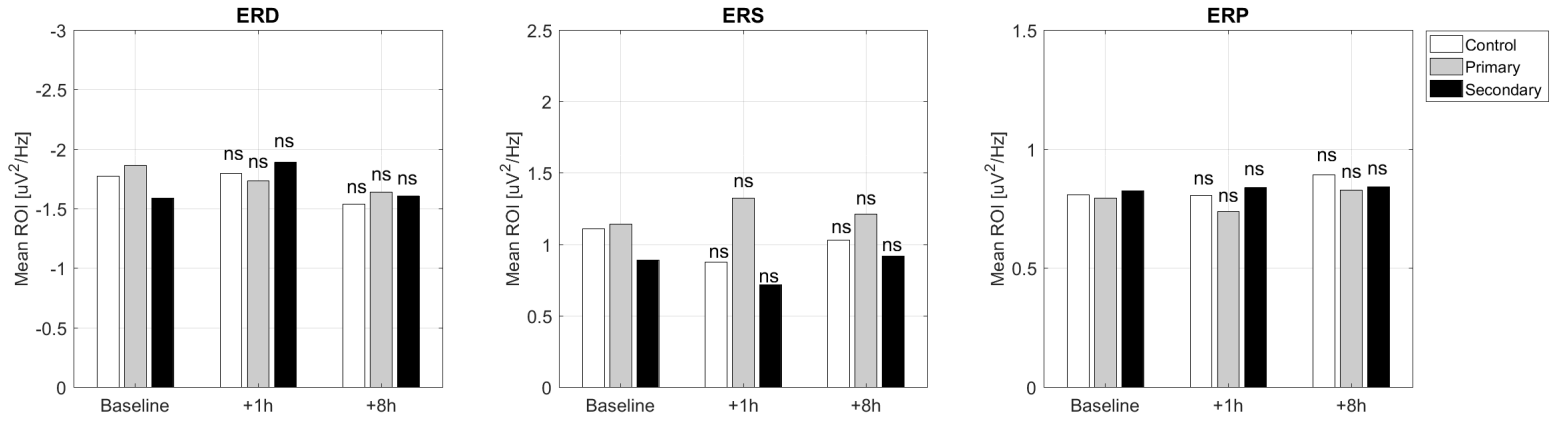
Type I - 1.00 mA

Figure 14: TF-ROIs for single pulse stimulation per area per measurement. TF-ROIs represents the mean of the bottom 20% (ERD) or top 20% (ERS, ERP) within a prespecified region of interest on the TFR. Significant differences between baseline and +1h, +8h measurements are depicted by asterisk (p≥.05=ns, p<.05=*, p<.01=**, p<.001=***). Notice the inverted vertical axes for ERD. ERD = event-related desynchronization, ERS = event-related synchronization, ERP = event-related potential, TF-ROI = time-frequency region of interest, TFR = time-frequency representation.

Type II - 0.50 mA
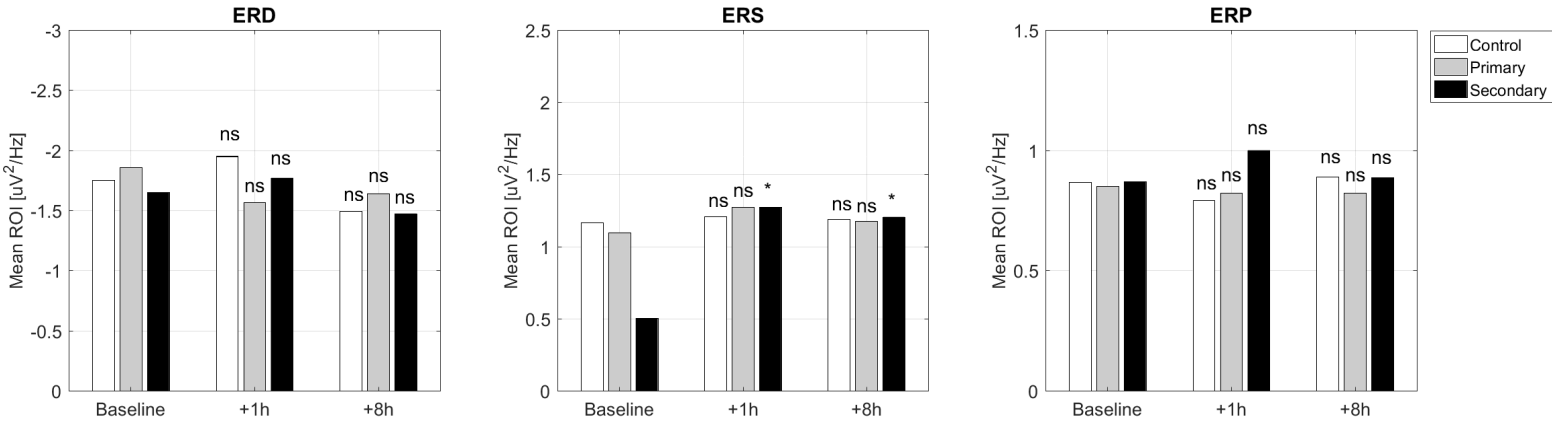
Figure 15: TF-ROIs for double pulse stimulation per area per measurement. TF-ROIs represents the mean of the bottom 20% (ERD) or top 20% (ERS, ERP) within a prespecified region of interest on the TFR. Significant differences between baseline and +1h, +8h measurements are depicted by asterisk (p≥.05=ns, p<.05=*, p<.01=**, p<.001=***). Notice the inverted vertical axes for ERD. ERD = event-related desynchronization, ERS = event-related synchronization, ERP = event-related potential, TF-ROI = time-frequency region of interest, TFR = time-frequency representation.

Discussion

**Conclusions:** The most important advantage of using LME models for EEG data analysis was the fact that all EEG trials could be included into one model. This made it possible to perform statistical analyses using all data sets and plot significance over time. In addition, combining psychophysical elements with phase locked EEG data showed the impact of stimulus detection, stimulus amplitude and number of pulses on EP amplitudes. The novel LME modeling method could be used to control these psychophysical elements in both phase locked and non-phase locked EEG analyses. For this study, capsaicin was used to challenge the novel method. The goal was to quantify peripheral and central sensitization effects using phase locked and non-phase locked analyses. Although the novel LME method could be used to find significant differences while controlling for psychophysical elements, attention and learning effects of the subjects probably played a role in the interpretation of the results. Desensitization after capsaicin application was particularly prominent in the psychophysical data and the phase locked EEG data. In contrast, ERS in the alpha band (8-11 Hz) showed sensitization effects in the secondary area and thus might be used as a predictor for central sensitization. However, more research is needed to support this conclusion.

EEG analysis methods comparison: averaging vs linear mixed-effect models

In this study, time-domain averaging of EPs resulted in more than 80% of the data showing no identifiable peaks (Fig 9b). This implied that the limited amount of extractable parameters (less than 20%) made ordinary statistical analyses (e.g. ANOVA) impossible. Four reasons could explain this large amount of noisy data. Firstly, IES stimulated in this experiment at relatively low stimulus intensities compared to other stimulation techniques (e.g. laser). Since the EP amplitude depended on the intensity of the stimulus, this ultimately resulted in low signal amplitudes. This can be supported by the low SNR over time (max: 0.0518) using the LME model describing stimulus detection as example (Fig 16). Secondly, not every stimulus was detected and therefore flattened out the average. Removing the not-detected stimuli from a data set resulted often in a loss of too many single trials to obtain a useful average (<20 trials). Thirdly, the stimulus amplitudes during Part I were fluctuating too much and therefore were not ideal for averaging. Finally, many data sets were composed of trials containing artefacts which after exclusion resulted again in a loss of too many single trials to obtain a useful average. Therefore, it was necessary in this experiment to use LME models to reduce the loss of information caused by averaging.

By including all trials in a LME model, averaging per data set was not needed to extract parameters for ANOVA analyses. Statistical analyses could be performed by means of post hoc contrast tests on the fixed effects of the LME models including all data. In case of the phase locked analyses, contrast tests were performed on each time point, revealing significant differences between contrasts on EP amplitudes over time. This not only gave information about significant effects between peak amplitudes, but also about the development of the peak over time. An example would be Fig 11a in which not only the peak amplitude, but also the time range of significance between a detected or not-detected response was
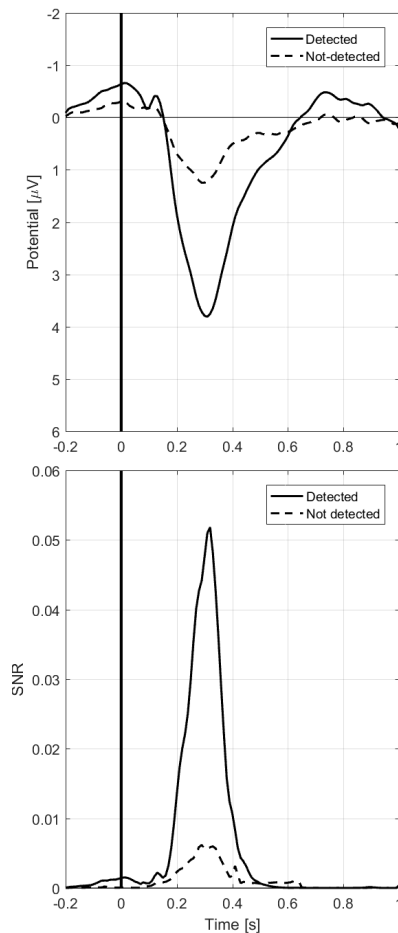

Figure 16: **Top:** *Effect of stimulus detection on EP amplitudes, see Fig 11a.* **Bottom:** *Signal-to-noise ratio (SNR) of EP amplitudes for detected and not-detected stimuli over time. Notice the increase in SNR during the P300 peak.*

20

quantified. Another example is Fig 11c, where according to ordinary time-domain averaging only a peak amplitude effect would be noticed. These LME models also showed different peak development characteristics between a single pulse or double pulse at 0.50 mA. A slightly faster onset of peak rise and peak decline could be deducted from the significant effects on the peak amplitudes. The extra information on the development of a peak over time might give new insights into the effect of interventions on the characteristics of EPs and therefore pain processing in general.

Psychophysical characteristics and effects on phase locked EEG data

Stimulus type on the psychophysical curve - see Fig 7
The detection thresholds for both single (0.61 mA) and double pulse (0.30 mA) stimulation were comparable to detection thresholds found by others, e.g. single pulses by Doll et al. (0.55 mA) [31], by van der Heide et al. (0.47 mA) [12] and double pulses by Doll et al. (0.31 mA) [31]. In addition, the slopes of single pulse (10.71 mA^{-1}) and double pulse (22.76 mA^{-1}) were also comparable to the results published by Doll et al. (9.54 mA^{-1} and 15.91 mA^{-1} respectively) [31]. This supports the validity of the psychophysical results.

Stimulus detection on the EP amplitude - see Fig 11a
The most prominent effect of combining the psychophysical data on the EP amplitudes was the effect of stimulus detection, whether the electrical stimulus was felt or not. This was expected, because EP amplitudes are related to stimulus processing [26]. Therefore, if a stimulus is not detected, no EP would be expected. However, a small EP remains visible for not-detected stimuli as well. A possible explanation for this phenomenon could be indecisiveness of the subject to indicate the stimulus being felt. IES stimulates at relatively low currents around the detection threshold, thereby constantly balancing on the edge of detection. Therefore, very weak stimuli might not be judged as detected by the subject, but could still be processed in the cortex.

Less expected are the significant differences between a detected and not-detected stimulus prestimulus and around 700-900 ms. Prestimulus differences would mean that signal processing occurred before the stimulus was given and therefore the body could anticipate the random stimulus selection procedure. However, a more plausible argument would be that these significant differences could be related to the EEG band pass filter settings (0.5-30 Hz). Distortions could have been amplified by the cut off value at 0.5 Hz, showing these biased results [32, 33]. This is supported by the low SNR prestimulus and around 700-900 ms (Fig 16). Therefore, these significant differences were probably related to filtering instead of stimulus detection.

Stimulus amplitude on EP amplitude - see Fig 11b
Significant increases in EP amplitude were found in the rising part of the P300 peak (0.13-0.24s). It seemed that increasing the stimulus amplitude resulted in an increase in EP amplitude combined with a decrease in peak latency (Fig 11b). The increase in EP amplitude was expected due to a larger stimulus intensity which resulted in a more painful experience. This effect had been reported by Mouraux et al. and Iwabe et al. before [10, 13], both showing increased EP amplitudes with increased stimulus amplitudes. The possible reduced latency could be explained by the fact that a larger stimulus amplitude depolarized the peripheral membrane faster. Finally, increasing the stimulus amplitude showed more high frequency oscillations. This was probably due to a lack of information at high stimulus amplitudes, resulting in a more noisy output. Therefore, increasing the stimulus amplitude resulted in an increase in energy transfer and consequently led to an increase in EP amplitude and possible decrease in peak latency.

Stimulus type on EP amplitude - see Fig 11c & 11d
Significant effects on the EP amplitude were found for the stimulus type when the stimulus amplitude was fixed, e.g. at 0.50 mA (Fig 11c). Increasing the number of pulses (NoP) resulted in an increase in EP amplitude in the rising part of the P300 peak (0.17-0.25s) and significant decrease in the EP amplitude in the declining part of the P300 peak (0.38-0.42s). The increase in peak amplitude is supported by Heide et al. who compared single pulse and multiple pulse stimulation [12]. They showed that increasing the NoP up to five pulses, accounted for increased N150-P300 amplitudes. Since a double pulse activated more afferents, the peak amplitude was increased.

On the other hand, differences in peak latencies due to multiple pulse stimulation have not been reported before. Since the double pulse consisted of a 10 ms inter-pulse interval, this could not be explained by the fact that a larger stimulus intensity depolarized the peripheral membrane faster. Perhaps the reduced latency could be explained by the fact that a larger stimulus intensity increased the priority of the stimulus in the central nervous system. This could be caused by a reduction in 'waiting time' between activation of the secondary neuron and further signal processing in the cortex. Moreover, the EP amplitude showed no reduction in latency when the stimulus amplitude was corrected for detection threshold (Fig 11d). Although double pulse stimulation stimulated at lower stimulus amplitudes than single pulse stimulation, both showed comparable EPs. Therefore, the perceived stimulus intensity could be considered as the main factor driving the EP characteristics.

From Fig 11a, 11b and 11c can be concluded that stimulus detection, stimulus amplitude and number of pulses may contribute significantly to the amplitude of EPs. To be able to investigate specific interventions on pain processing using EEG methods while controlling psychophysical elements, it was necessary to combine them in a LME model. The models were able to integrate the psychophysical data with the EEG data and were used to find significant differences. To challenge this analysis method, capsaicin was applied to the skin to induce sensitization effects which were to be detected by LME models.

Detecting sensitization effects induced by capsaicin

Psychophysical data - see Fig 8
Decreases in detection threshold were expected due to known sensitization effects of capsaicin [34, 35, 36]. However, only increases in detection threshold were found for both single and double pulse stimuli. This pattern of apparent desensitization could have had several causes. First, a learning effect might be present. The first measurement for every subject was the baseline measurement at secondary area. This measurement showed the lowest detection thresholds for both stimulus types, indicating that the first measurement was the most sensitive for the detection threshold. Second, lack of attention might have played a role in the increasing thresholds as well. A single stimulation block lasted for 45 minutes and the occasion lasted 14 hours in total[21]. This is supported by the trends in detection thresholds within each measurement block. Since the measurement sequence was not randomized (Secondary - Control - Primary), increasing trends could be noticed within each measurement block from the secondary to the primary area. Therefore, psychophysical results related to single pulse stimulation were probably affected by attention and learning effects.

Interestingly, the double pulse stimulation showed increased thresholds for the primary and secondary area, but did not show significantly increased detection thresholds over time for the control location. This would imply that capsaicin itself had a desensitizing effect on the psychophysical curve. Since double pulse stimulation induced facilitatory processes (see Fig 7), it might have competed with capsaicin its sensitization effects. This could be supported by the fact that IES stimulated Aδ-fibers which were targeted by capsaicin as well [10]. Further research is necessary that could support this conclusion. Therefore, an pain facilitation analysis is proposed in the Future recommendations: psychophysical analyses.

EEG - Phase locked analyses - see Fig 10, 12 & 13
In this study, we analyzed the EPs using time-domain averaging and LME modeling. Time-domain averaging resulted in only 14% of the data sets with visually distinguishable N150-P300 peaks (Fig 9). Therefore, performing a statistical analysis on the effect of capsaicin was difficult. On the other hand, time-domain averaging was useful to visualize grand averages, which indicated decreased EP amplitudes after capsaicin application (Fig 10). However, to perform statistical analyses LME models were necessary.

Fig 12 & 13 show the EPs over time at fixed stimulus amplitudes for both single (1.00 mA) and double (0.50 mA) pulse stimulation. Due to the inclusion of all trials, the LME models were sensitive to very small changes (< 0.1 mA). In this study, the single pulse stimulation showed overall desensitization ef-

---

[21]For more information see Appendix V: Schedule of Assessments

fects after baseline. The most prominent and long lasting decreases were visible 8 hours after capsaicin application and were probably related to lack of attention [37]. Remarkably, the double pulse stimulation showed strongest desensitization effects in the secondary area. Probably, learning effects played a comparable role in desensitization related to the detection thresholds. Therefore, the phase locked EEG data is comparable to the psychophysical results, both being affected by attention and learning effects. Since the phase locked analyses could have been biased by across-trial latency-jitter, non-phase locked analyses were performed as well.

EEG - Non-phase locked analyses - see Fig 14 & 15
Non-phase locked analyses made it possible to investigate transient modulations of power within a pre-specified ROI. Changes in alpha rhythms could have been modulated by bottom-up sensory inputs and top-down cognitive modulation. A suppression in ERD power can either be explained by exogenous activation of the primary sensory cortex induced by noxious stimuli [38, 39] or by endogenous voluntary orienting of attention to noxious stimulation [40, 30]. Since the former is mainly observed at the central electrodes and the latter at the posterior parietal and occipital electrodes [30], our negative ERD power values might be related to the exogenous activation due to electrical stimulation. Unfortunately, capsaicin did not show any significant effects on the ERD power for both stimulus types on all areas. This means that the ERD power in the alpha band due to exogenous activation was not influenced by capsaicin application using the current analysis method.

Capsaicin did show significant increases in ERS power in the alpha band for double pulse stimulation in the secondary area (Fig 15). ERS power is thought to reflect processes of active cortical inhibition [41]. However, these responses rely mainly on long-lasting periods in brain regions that are not related to the central midline electrode. Therefore, it is unlikely our increase in ERS power corresponded to cortical deactivation patterns. Mouraux et al. discussed that ERS power in this ROI could resemble an EP in the alpha band which was subject to latency-jitter [42]. This possible non-phase locked EP was of a faster and higher frequency type than the conventional phase locked EP in the ERP ROI. Perhaps this 'special' EP was influenced by latency-jitter and was sensitive to capsaicin application. Since it showed an increase in power after capsaicin application in the secondary area, it could serve as a quantifier in detecting central sensitization.

ERP power reflected the phase locked EPs including latency-jitter. Although no significant effects were found, ERP power values did show elevated instead of reduced trends for the double pulse stimulation for the secondary area, which could indicate central sensitization effects. Capsaicin might have affected the latencies of the P300 peaks in such a way that the phase locked analyses showed biased decreases in amplitude[22]. However, the increase of ERS power and ERP power were relatively small and no increases were found for single pulse stimulation or within the primary area. Therefore, more studies using IES in combination with capsaicin sensitization and non-phase locked analyses are needed to support these conclusions.

Future recommendations

Experimental setup
Five recommendations to optimize the current experimental setup are considered. First, a reduction in stimulation time is necessary to account for a lack of attention. This can be done by removing Part I (psychophysical parameter estimation) after the baseline measurement or removing the single pulse. Removing Part I will reduce the stimulation time from 45 to 24 minutes and choosing the double pulse will reduce the stimulation time from 45 to 22.5 minutes. Secondly, an initial test round should be implemented to minimize possible learning effects. Since the baseline measurement for the secondary area was always the most sensitive (lowest detection threshold and largest EP amplitude), learning effects could have influenced the results. Thirdly, the stimulation areas should be randomized. In this study, we chose to perform the stimulation on the areas in the same consecutive order due to logistical reasons (Secondary - Control - Primary). Therefore, time effects could not have been separated from the effect of the area. Fourthly, for each measurement the stimulus amplitudes in Part II were based on

---

[22]For more information see Appendix IV: Non-phase locked analyses

the detection threshold determined in Part I. However, to find effects of the intervention, the stimulus amplitudes in Part II after intervention should have been the same as the stimulus amplitudes in Part II before the intervention. LME models were able to correct for this by fixing the stimulus amplitude, but the quality of the data would have been better if this had been implemented in the experimental setup. Finally, changing the stimulus characteristics of IES might shift the preference of activation from Aδ-fibers to C-fibers [43, 7]. Since capsaicin activates TRPV1 channels that can be found primarily on C-fibers, peripheral sensitization might show up more easily with IES using C-fiber stimulus characteristics.

Psychophysical analyses

Differences in detection thresholds are influenced by the number of pulses [12]. In our study, double pulse stimulation showed effects on the detection threshold and slope of the psychophysical curve. Moreover, the observed double pulse stimulation resulted in lower detection thresholds compared to the expected double pulse stimulation based on pure probability summation (Fig 7). Therefore, some form of facilitatory processes must have accounted for the extra decrease in detection threshold. Since capsaicin is expected to induce sensitization effects, single and double pulse stimulation could be used to identify the effect of pain facilitation within each stimulation area, thereby reducing attention or learning effects. These facilitatory processes could be quantified by the ratio of detection thresholds, suggested as the pain facilitation ratio (PFR, see Eq 3 and Fig 17).

$$PFR = \frac{\alpha_s - \alpha_d}{\alpha_s - \alpha_p} - 1 \tag{3}$$

with α_s = detection threshold of a single pulse, α_d = detection threshold of a double pulse and α_p = detection threshold of the pure probability summation.
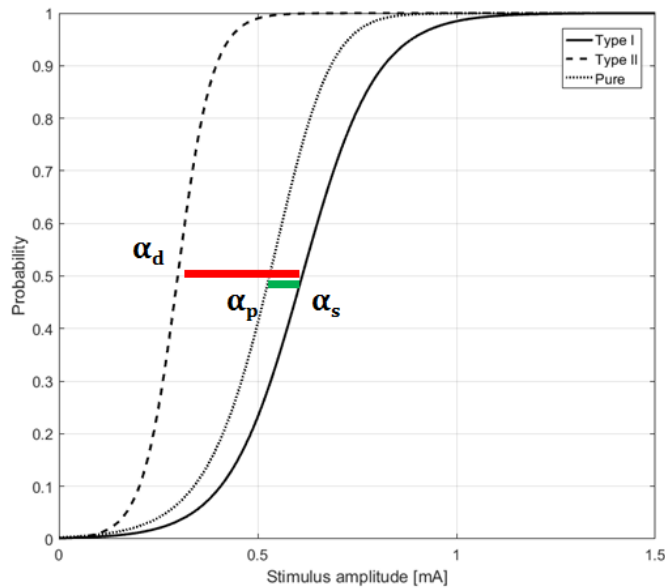

Figure 17: Facilitatory process visualized. The ratio between detection thresholds $(\alpha_s - \alpha_d)/(\alpha_s - \alpha_p) - 1$ might be useful as an indicator to describe pain facilitatory processes. When there is no difference in detection threshold between the observed and the expected double pulse, the PFR = 0. When there the observed double pulse has a detection threshold lower than the expected double pulse, the PFR is positive and vice versa.

Phase locked analyses

Four future recommendations can be considered regarding the phase locked analyses. First, no correction was applied to the p-values over time. A commonly used method to correct for multiple comparisons is the Bonferonni correction [44]. The Bonferonni method corrects by testing each individual hypothesis at a significance level of $\frac{\alpha}{m}$, with α being the desired overall significance and m the number of hypotheses. This method was not applicable in our situation, due to the fact that the total number of hypotheses was based on an adaptable sample frequency and trial length. Therefore, we suggest another type of

correction method based on consecutive significant differences over time. Since comparable P300 peaks are expected, significant differences are expected to be connected over time. Therefore, filtering out non-consecutive p-values for $x\%$ of the peak width could resolve the correction problem. Secondly, attention could be modeled within the LME model. Since attention is dependent on stimulus intensity and time, the model could incorporate a continuous attention variable based on amplitude over time (e.g. `Attention = Stim/Time`) within each stimulation block. Thirdly, the EEG filtering could be optimized. The FieldTrip package first defines the trials and subsequently filters the trials. This resulted in edge effects due to the high pass filter settings. Filtering first and subsequently defining trials could reduce these edge effects. Finally, the artefacts were automatically removed by automatic rejection of trials containing potentials larger than 4 times the standard deviation. More complex techniques, such as independent component analysis (ICA) [45] or blind source separation (BSS) [46], could be used to correct for artefacts instead of rejecting trials.

Non-phase locked analyses
In this study, mean power values of top or bottom 20% TF-ROIs were used as endpoints in the LME model to study non-phase locked effects. Although across-trial variability was included, averaging the power values within each ROI led to a substantial loss of information. To get a better understanding on the behavior of TF-ROIs after intervention, LME models could be used to model each power value in the entire TFR. This also gives the possibility to test which area within the TF-ROI is significantly different. Although it extends the problem of correcting for p-values over time-frequency regions, it might reveal new regions of interest.

The final recommendation is to analyze the gamma band (30-100 Hz) information. ERS in the gamma band is thought to play an important role in cortical integration and perception [47, 48]. Moreover, Zhang et al. emphasized the fact that gamma band oscillations induced by laser stimulations are closely related to pain perception while being independent of stimulus saliency [49]. Therefore, this endpoint could be included in a LME TFR model to avoid possible effects of attention.

References

[1] F. Frolund and C. Frolund, "Pain in general practice. Pain as a cause of patient-doctor contact.," *Scandinavian journal of primary health care*, vol. 4, pp. 97–100, 5 1986.

[2] O. Gureje, M. Von Korff, G. E. Simon, and R. Gater, "Persistent pain and well-being: a World Health Organization Study in Primary Care.," *JAMA*, vol. 280, pp. 147–51, 7 1998.

[3] P. Mäntyselkä, E. Kumpusalo, R. Ahonen, A. Kumpusalo, J. Kauhanen, H. Viinamäki, P. Halonen, and J. Takala, "Pain as a reason to visit the doctor: a study in Finnish primary health care.," *Pain*, vol. 89, pp. 175–80, 1 2001.

[4] B. Sessle, "Unrelieved pain: a crisis.," *Pain research & management*, vol. 16, no. 6, pp. 416–20, 2011.

[5] M. Curatolo, S. Petersen-Felix, and L. Arendt-Nielsen, "Sensory assessment of regional analgesia in humans: a review of methods and applications.," *Anesthesiology*, vol. 93, pp. 1517–30, 12 2000.

[6] L. Petrini, K. Hennings, X. Li, F. Negro, and L. Arendt-Nielsen, "A human experimental model of episodic pain," *International Journal of Psychophysiology*, vol. 94, pp. 496–503, 12 2014.

[7] J. Motogi, M. Kodaira, Y. Muragaki, K. Inui, and R. Kakigi, "Cortical responses to C-fiber stimulation by intra-epidermal electrical stimulation: An MEG study," *Neuroscience Letters*, vol. 570, pp. 69–74, 2014.

[8] P. Steenbergen, J. R. Buitenweg, J. Trojan, E. M. van der Heide, T. van den Heuvel, H. Flor, and P. H. Veltink, "A system for inducing concurrent tactile and nociceptive sensations at the same site using electrocutaneous stimulation.," *Behavior research methods*, vol. 44, pp. 924–33, 12 2012.

[9] K. Inui, T. Tran, Y. Qiu, X. Wang, and M. Hoshiyama, "Pain-related magnetic fields evoked by intra-epidermal electrical stimulation in humans," *Clinical*, 2002.

[10] A. Mouraux, G. D. Iannetti, and L. Plaghki, "Low intensity intra-epidermal electrical stimulation can activate Adelta-nociceptors selectively," *Pain*, vol. 150, no. 1, pp. 199–207, 2010.

[11] F. Kingdom and N. Prins, *Psychophysics: A Practical Introduction*, vol. 53. 2013.

[12] E. M. van der Heide, J. R. Buitenweg, E. Marani, and W. L. C. Rutten, "Single Pulse and Pulse Train Modulation of Cutaneous Electrical Stimulation: A Comparison of Methods," *Journal of Clinical Neurophysiology*, vol. 26, pp. 54–60, 2 2009.

[13] T. Iwabe, I. Ozaki, and A. Hashizume, "The respiratory cycle modulates brain potentials, sympathetic activity, and subjective pain sensation induced by noxious stimulation.," *Neuroscience research*, vol. 84, pp. 47–59, 7 2014.

[14] M. Liang, M. C. Lee, J. O'Neill, A. H. Dickenson, and G. D. Iannetti, "Brain potentials evoked by intraepidermal electrical stimuli reflect the central sensitization of nociceptive pathways," vol. 116, pp. 286–295, 8 2016.

[15] N. Otsuru, K. Inui, K. Yamashiro, T. Miyazaki, Y. Takeshima, and R. Kakigi, "Assessing A?? Fiber Function With Lidocaine Using Intraepidermal Electrical Stimulation," *Journal of Pain*, vol. 11, no. 7, pp. 621–627, 2010.

[16] R. J. Doll, *Psychophysical methods for improved observation of nociceptive processing*. PhD thesis, Twente University, 2016.

[17] R. J. Doll, P. H. Veltink, and J. R. Buitenweg, "Observation of time-dependent psychophysical functions and accounting for threshold drifts," 2015.

[18] G. A. Gescheider, M. E. Berryhill, R. T. Verrillo, and S. J. Bolanowski, "Vibrotactile temporal summation: probability summation or neural integration?," *Somatosensory & motor research*, vol. 16, no. 3, pp. 229–42, 1999.

[19] R. J. Doll, J. R. Buitenweg, H. G. E. Meijer, and P. H. Veltink, "Tracking of nociceptive thresholds using adaptive psychophysical methods," *Behavior Research Methods*, vol. 46, no. 1, pp. 55–66, 2014.

[20] V. Legrain, G. D. Iannetti, L. Plaghki, and A. Mouraux, "The pain matrix reloaded: A salience detection system for the body," *Progress in Neurobiology*, vol. 93, no. 1, pp. 111–124, 2011.

[21] A. Mouraux, E. Marot, and V. Legrain, "Short trains of intra-epidermal electrical stimulation to elicit reliable behavioral and electrophysiological responses to the selective activation of nociceptors in humans," *Neuroscience Letters*, vol. 561, pp. 69–73, 2014.

[22] L. Hu, Z. G. Zhang, A. Mouraux, and G. D. Iannetti, "Multiple linear regression to estimate time-frequency electrophysiological responses in single trials," *NeuroImage*, vol. 111, pp. 442–453, 2015.

[23] V. V. Nikulin, K. Linkenkaer-Hansen, G. Nolte, S. Lemm, K. R. Müller, R. J. Ilmoniemi, and G. Curio, "A novel mechanism for evoked responses in the human brain," *European Journal of Neuroscience*, vol. 25, pp. 3146–3154, 6 2007.

[24] A. Mazaheri and O. Jensen, "Asymmetric amplitude modulations of brain oscillations generate slow evoked responses.," *The Journal of neuroscience : the official journal of the Society for Neuroscience*, vol. 28, pp. 7781–7, 7 2008.

[25] M. Schooneman, *Measurement of evoked potentials during multiple threshold tracking of nociceptive electrocutaneous stimuli.* PhD thesis, TU Twente, 2015.

[26] L. Garcia-Larrea, "Chapter 30 Evoked potentials in the assessment of pain," *Pain*, vol. 81, pp. 439 – 462, X–XI, 2006.

[27] A. Mouraux and G. Iannetti, "Across-trial averaging of event-related EEG responses and beyond," *Magnetic Resonance Imaging*, vol. 26, pp. 1041–1054, 9 2008.

[28] S. F. Pedersen, G. Owsianik, and B. Nilius, "TRP channels: An overview," *Cell Calcium*, vol. 38, pp. 233–252, 9 2005.

[29] R. Oostenveld, P. Fries, E. Maris, and J.-M. Schoffelen, "FieldTrip: Open Source Software for Advanced Analysis of MEG, EEG, and Invasive Electrophysiological Data," *Computational Intelligence and Neuroscience*, vol. 2011, pp. 1–9, 2011.

[30] L. Hu, W. Peng, E. Valentini, Z. Zhang, and Y. Hu, "Functional features of nociceptive-induced suppression of alpha band electroencephalographic oscillations," *The Journal of Pain*, 2013.

[31] R. J. Doll, A. C. A. Maten, S. P. G. Spaan, P. H. Veltink, and J. R. Buitenweg, "Effect of temporal stimulus properties on the nociceptive detection probability using intra-epidermal electrical stimulation," *Experimental Brain Research*, vol. 234, pp. 219–227, 1 2016.

[32] D. J. Acunzo, G. MacKenzie, and M. C. W. van Rossum, "Systematic biases in early ERP and ERF components as a result of high-pass filtering," *Journal of Neuroscience Methods*, vol. 209, no. 1, pp. 212–218, 2012.

[33] D. Tanner, K. Morgan-Short, and S. J. Luck, "How inappropriate high-pass filters can produce artifactual effects and incorrect conclusions in ERP studies of language and cognition," *Psychophysiology*, vol. 52, no. 8, pp. 997–1009, 2015.

[34] J. Dirks, K. L. Petersen, and J. B. Dahl, "The heat/capsaicin sensitization model: a methodologic study.," *The journal of pain : official journal of the American Pain Society*, vol. 4, pp. 122–8, 4 2003.

[35] K. L. Petersen, B. Jones, V. Segredo, J. B. Dahl, and M. C. Rowbotham, "Effect of remifentanil on pain and secondary hyperalgesia associated with the heat–capsaicin sensitization model in healthy volunteers.," *Anesthesiology*, vol. 94, pp. 15–20, 1 2001.

[36] G. C. Scanlon, M. S. Wallace, S. J. Ispirescu, and G. Schulteis, "Intradermal Capsaicin Causes Dose-Dependent Pain, Allodynia, and Hyperalgesia in Humans," *Journal of Investigative Medicine*, vol. 54, pp. 238–244, 7 2006.

[37] R. D. Treede, J. Lorenz, and U. Baumgärtner, "Clinical usefulness of laser-evoked potentials," *Neurophysiologie Clinique*, vol. 33, no. 6, pp. 303–314, 2003.

[38] M. Ploner, J. Gross, L. Timmermann, B. Pollok, and A. Schnitzler, "Oscillatory activity reflects the excitability of the human somatosensory system," *NeuroImage*, vol. 32, pp. 1231–1236, 9 2006.

[39] S. Ohara, N. Crone, N. Weiss, and F. Lenz, "Attention to a painful cutaneous laser stimulus modulates electrocorticographic event-related desynchronization in humans," *Clinical Neurophysiology*, vol. 115, pp. 1641–1652, 7 2004.

[40] G. D. Iannetti, N. P. Hughes, M. C. Lee, and A. Mouraux, "Determinants of Laser-Evoked EEG Responses: Pain Perception or Stimulus Saliency?," *Journal of Neurophysiology*, vol. 100, pp. 815–828, 6 2008.

[41] G. Pfurtscheller and F. Lopes da Silva, "Event-related EEG/MEG synchronization and desynchronization: basic principles," *Clinical Neurophysiology*, vol. 110, pp. 1842–1857, 11 1999.

[42] A. Mouraux, J. M. Guérit, and L. Plaghki, "Non-phase locked electroencephalogram (EEG) responses to CO2 laser skin stimulations may reflect central interactions between A partial partial differential- and C-fibre afferent volleys.," *Clinical neurophysiology : official journal of the International Federation of Clinical Neurophysiology*, vol. 114, pp. 710–22, 4 2003.

[43] N. Otsuru, K. Inui, K. Yamashiro, and T. Miyazaki, "Selective stimulation of C fibers by an intra-epidermal needle electrode in humans," *Open Pain*, 2009.

[44] R. A. Armstrong, "When to use the Bonferroni correction," *Ophthalmic and Physiological Optics*, vol. 34, pp. 502–508, 9 2014.

[45] A. Hyvärinen and E. Oja, "Independent Component Analysis: Algorithms and Applications," vol. 13, no. 4–5, pp. 411–430, 2000.

[46] N. Oosugi, K. Kitajo, N. Hasegawa, Y. Nagasaka, K. Okanoya, and N. Fujii, "A new method for quantifying the performance of EEG blind source separation algorithms by referencing a simultaneously recorded ECoG signal.," *Neural networks : the official journal of the International Neural Network Society*, vol. 93, pp. 1–6, 9 2017.

[47] P. Fries, "Neuronal Gamma-Band Synchronization as a Fundamental Process in Cortical Computation," *Annual Review of Neuroscience*, vol. 32, pp. 209–224, 6 2009.

[48] E. Valentini, V. Betti, L. Hu, and S. M. Aglioti, "Hypnotic modulation of pain perception and of brain activity triggered by nociceptive laser stimuli.," *Cortex; a journal devoted to the study of the nervous system and behavior*, vol. 49, pp. 446–62, 2 2013.

[49] Z. G. Zhang, L. Hu, Y. S. Hung, A. Mouraux, and G. D. Iannetti, "Gamma-Band Oscillations in the Primary Somatosensory Cortex–A Direct and Obligatory Correlate of Subjective Pain Intensity," *Journal of Neuroscience*, vol. 32, no. 22, pp. 7429–7438, 2012.

[50] M. R. Mulvey, M. I. Bennett, I. Liwowsky, and R. Freynhagen, "The role of screening tools in diagnosing neuropathic pain," *Pain Management*, vol. 4, pp. 233–243, 5 2014.

[51] R. C. W. Jones and M. M. Backonja, "Review of neuropathic pain screening and assessment tools.," *Current pain and headache reports*, vol. 17, p. 363, 9 2013.

[52] K. Meacham, A. Shepherd, D. P. Mohapatra, and S. Haroutounian, "Neuropathic Pain: Central vs. Peripheral Mechanisms," *Current Pain and Headache Reports*, vol. 21, p. 28, 6 2017.

[53] S. Landy, "Migraine Headaches and Allodynia: Early Use of Triptans to Improve Outcome."

[54] C. Domnick, M. Hauck, K. L. Casey, A. K. Engel, and J. Lorenz, "C-fiber-related EEG-oscillations induced by laser radiant heat stimulation of capsaicin-treated skin.," *Journal of pain research*, vol. 2, pp. 49–56, 3 2009.

[55] A. Z. Tzabazis, M. Klukinov, S. Crottaz-Herbette, M. I. Nemenov, M. S. Angst, and D. C. Yeomans, "Selective nociceptor activation in volunteers by infrared diode laser.," *Molecular pain*, vol. 7, p. 18, 3 2011.

[56] J. O'Neill, C. Brock, A. E. Olesen, T. Andresen, M. Nilsson, and A. H. Dickenson, "Unravelling the Mystery of Capsaicin: A Tool to Understand and Treat Pain," *Pharmacological Reviews*, vol. 64, pp. 939–971, 10 2012.

[57] R. Planells-Cases, N. Garcìa-Sanz, C. Morenilla-Palao, and A. Ferrer-Montiel, "Functional aspects and mechanisms of TRPV1 involvement in neurogenic inflammation that leads to thermal hyperalgesia," *Pflügers Archiv - European Journal of Physiology*, vol. 451, pp. 151–159, 10 2005.

[58] R. H. LaMotte, C. N. Shain, D. A. Simone, and E. F. Tsai, "Neurogenic hyperalgesia: psychophysical studies of underlying mechanisms," *Journal of Neurophysiology*, vol. 66, no. 1, 1991.

[59] A. L. Oaklander, K. Romans, S. Horasek, A. Stocks, P. Hauer, and R. A. Meyer, "Unilateral postherpetic neuralgia is associated with bilateral sensory neuron damage," *Annals of Neurology*, vol. 44, pp. 789–795, 11 1998.

[60] K. L. Petersen, F. L. Rice, M. Farhadi, H. Reda, and M. C. Rowbotham, "Natural history of cutaneous innervation following herpes zoster," *Pain*, vol. 150, pp. 75–82, 7 2010.

[61] M. Ragé, N. Acker, M. W. M. Knaapen, M. Timmers, J. Streffer, M. P. Hermans, C. Sindic, T. Meert, and L. Plaghki, "Asymptomatic small fiber neuropathy in diabetes mellitus: investigations with intraepidermal nerve fiber density, quantitative sensory testing and laser-evoked potentials," *Journal of Neurology*, vol. 258, pp. 1852–1864, 10 2011.

[62] C.-C. Chao, M.-T. Tseng, Y.-J. Lin, W.-S. Yang, S.-C. Hsieh, Y.-H. Lin, M.-J. Chiu, Y.-C. Chang, and S.-T. Hsieh, "Pathophysiology of Neuropathic Pain in Type 2 Diabetes: Skin denervation and contact heat-evoked potentials," *Diabetes Care*, vol. 33, pp. 2654–2659, 12 2010.

[63] L. Zhou, D. W. Kitch, S. R. Evans, P. Hauer, S. Raman, G. J. Ebenezer, M. Gerschenson, C. M. Marra, V. Valcour, R. Diaz-Arrastia, K. Goodkin, L. Millar, S. Shriver, D. M. Asmuth, D. B. Clifford, D. M. Simpson, J. C. McArthur, and NARC and ACTG A5117 Study Group, "Correlates of epidermal nerve fiber densities in HIV-associated distal sensory polyneuropathy," *Neurology*, vol. 68, pp. 2113–2119, 6 2007.

[64] M. Polydefkis, C. T. Yiannoutsos, B. A. Cohen, H. Hollander, G. Schifitto, D. B. Clifford, D. M. Simpson, D. Katzenstein, S. Shriver, P. Hauer, A. Brown, A. B. Haidich, L. Moo, and J. C. McArthur, "Reduced intraepidermal nerve fiber density in HIV-associated sensory neuropathy.," *Neurology*, vol. 58, pp. 115–9, 1 2002.

[65] L. J. Scott, J. W. Griffin, C. Luciano, N. W. Barton, T. Banerjee, T. Crawford, J. C. McArthur, A. Tournay, and R. Schiffmann, "Quantitative analysis of epidermal innervation in Fabry disease.," *Neurology*, vol. 52, pp. 1249–54, 4 1999.

[66] P. Tympanidis, G. Terenghi, and P. Dowd, "Increased innervation of the vulval vestibule in patients with vulvodynia.," *The British journal of dermatology*, vol. 148, pp. 1021–7, 5 2003.

[67] P. Anand and K. Bley, "Topical capsaicin for pain management: therapeutic potential and mechanisms of action of the new high-concentration capsaicin 8% patch.," *British journal of anaesthesia*, vol. 107, pp. 490–502, 10 2011.

[68] N. Bohm-Starke, M. Hilliges, C. Falconer, and E. Rylander, "Increased intraepithelial innervation in women with vulvar vestibulitis syndrome.," *Gynecologic and obstetric investigation*, vol. 46, no. 4, pp. 256–60, 1998.

[69] Z. Yilmaz, T. Renton, Y. Yiangou, J. Zakrzewska, I. Chessell, C. Bountra, and P. Anand, "Burning mouth syndrome as a trigeminal small fibre neuropathy: Increased heat and capsaicin receptor TRPV1 in nerve fibres correlates with pain score," *Journal of Clinical Neuroscience*, vol. 14, pp. 864–871, 9 2007.

[70] M. Devor, "Sodium Channels and Mechanisms of Neuropathic Pain," *The Journal of Pain*, vol. 7, pp. S3–S12, 1 2006.

[71] L. J. Hudson, S. Bevan, G. Wotherspoon, C. Gentry, A. Fox, and J. Winter, "VR1 protein expression increases in undamaged DRG neurons after partial nerve injury," *European Journal of Neuroscience*, vol. 13, pp. 2105–2114, 6 2001.

[72] M. J. Craner, J. P. Klein, J. A. Black, and S. G. Waxman, "Preferential expression of IGF-I in small DRG neurons and down-regulation following injury.," *Neuroreport*, vol. 13, pp. 1649–52, 9 2002.

[73] R. Baron, "Neuropathic Pain: A Clinical Perspective," in *Handbook of experimental pharmacology*, no. 194, pp. 3–30, 2009.

[74] R. J. Doll, J. R. Buitenweg, H. G. E. Meijer, and P. H. Veltink, "Tracking of nociceptive thresholds using adaptive psychophysical methods," *Behavior Research Methods*, vol. 46, pp. 55–66, 3 2014.

[75] R. Doll, G. Amerongen, J. Hay, and G. Groeneveld, "Responsiveness of electrical nociceptive detection thresholds to capsaicin (8%)-induced changes in nociceptive processing," *Experimental brain*, 2016.

[76] A. B. Watson and A. Fitzhugh, "The method of constant stimuli is inefficient.," *Perception & psychophysics*, vol. 47, pp. 87–91, 1 1990.

[77] T. N. CORNSWEET, "The staircrase-method in psychophysics.," *The American journal of psychology*, vol. 75, pp. 485–91, 9 1962.

Appendix I: Neuropathic pain and capsaicin model

Pain is the most common reason for visiting a doctor and despite the fact that a large variety of analgesics exists on the pharmaceutical market, many pain symptoms remain unrelieved [4]. Pain can be categorized as nociceptive and neuropathic pain. Nociceptive pain arises due to the activation of nociceptors in the nervous system and it is caused by damage to non-neural tissue. Neuropathic pain arises due to a malfunction of the nervous system and it is often caused by a lesion or a disease affecting neural tissue [50]. Although many types of analgesics exist that are effective in the treatment of nociceptive pain, much improvement is still needed for the treatment of neuropathic pain. This is stressed by the fact that only 40-60% of patients that suffer neuropathic pain problems obtain relief, which is mostly partial relief only [51]. One way to solve this problem is to support drug development that specifically targets elements of neuropathic pain.

Human experimental pain models have been established to support drug development by inducing well-defined noxious stimuli in healthy individuals under controlled circumstances. This gives the possibility to investigate specific elements of the pain system without the influence of other unwanted (clinical) symptoms. Specific elements of neuropathic pain are peripheral and central sensitization [52]. Peripheral sensitization is caused by modulation of peripheral afferents, while central sensitization is caused by modulation of secondary neurons in the central nervous system. Both peripheral and central sensitization are characterized by a reduction in pain threshold (hyperalgesia). Peripheral sensitization is closely linked to the site of injury, i.e. primary hyperalgesia, while central sensitization can also be explained by a reduction in pain threshold surrounding the site of injury, i.e. secondary hyperalgesia. Therefore, development of a human experimental pain model that simulates peripheral and central sensitization by evoking primary and secondary hyperalgesia, may support drug development for neuropathic pain.
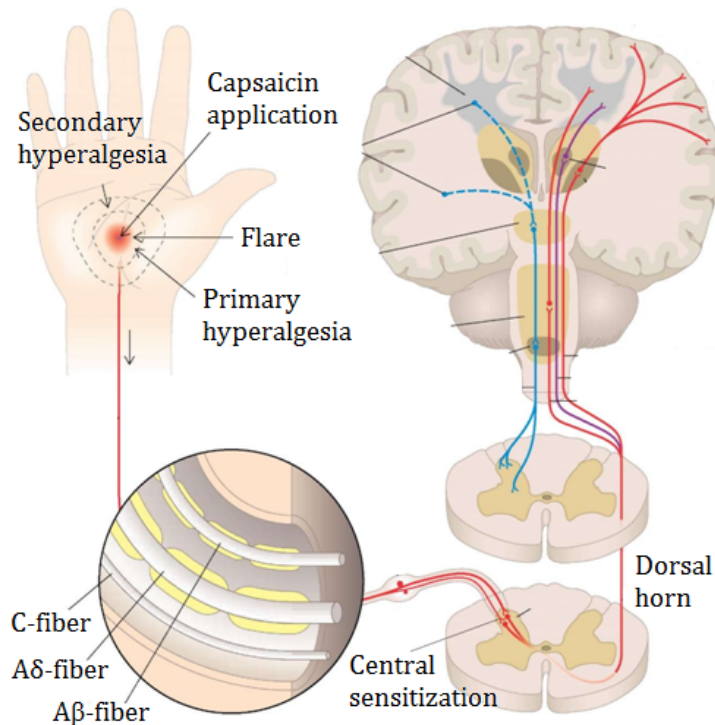

Figure 18: Capsaicin can be used in a human experimental pain model to induce sensitization effects related to neuropathic pain. Application to the skin may result in a reduction in pain threshold within the site of application, i.e. primary hyperalgesia, and a reduction in pain threshold surrounding the site of application, i.e. secondary hyperalgesia. Since peripheral sensitization is closely linked to primary hyperalgesia and central sensitization partly explained by secondary hyperalgesia, primary and secondary hyperalgesia areas can be used as proxy measures for peripheral and central sensitization. Illustration adapted from MedScape [53]

Capsaicin is a chemical compound that is often used to induce effects of peripheral and central sensitization (Fig 18) [14, 54, 55, 56]. It is a highly selective agonist for the vanniloid receptor 1 (TRPV1), which is an important transducer of noxious thermal and chemical evoked stimulations [28]. The direct activation of TRPV1 by capsaicin increases excitability of nociceptors, triggers the release of pro-inflammatory agents at peripheral terminals and sensitizes nociceptors, either by phosphorylation of or up-regulating intracellular signaling cascades. This feedback circuit contributes to enhance the hypersensitivity of inflamed tissue [57] and can result in peripheral sensitization. Central sensitization induced by capsaicin is thought to be caused by the tonic activity of peripheral afferents that in turn sensitize the secondary neurons in the spinal cord [58]. Due to the sensitization of these secondary neurons, incoming pain-related signals from the site surrounding the capsaicin application are enhanced at the dorsal horn. Therefore, capsaicin may be used to sensitize the pain system, simulating elements of neuropathic pain. Quantification of this sensitization can be done by stimulating the primary and secondary hyperalgesia areas and quantifying the related responses before and after capsaicin application.

Neuropathy in more detail

Most neuropathic pain syndromes are characterized by a decreased sensory neuron axonal density, but are often subject to increased peripheral sensitization caused by neurotrophins. Immunohistochemical analyses have shown that the intra-epidermal nerve fibre density (IENFD) is decreased in a wide range of neuropathic syndromes including postherpetic neuralgia (PHN) [59, 60], painful diabetic neuropathy (PDN) [61, 62], painful HIV-associated neuropathy [63, 64] and Fabry disease [65]. However, some other conditions such as vulvodynia [66] have an increased IENFD with hyperexcitability, induced by immune system activation. The hyperactivity of nociceptors in neuropathic syndromes is most likely due to an overstimulating environment to which intact or regenerating nociceptors are exposed [67].

Differences in skin innervation can be used to categorize the neuropathic pain syndromes of diverse etiologies; see Fig 19. According to Anand and Bley, three groups of neuropathic pain syndromes can be distinguished: static denervation neuropathy, dynamic denervation neuropathy and hyperinnervation neuropathy [67]. PHN is a static denervation neuropathy. When cell bodies are lost and cannot regrow, reduced innervation results in intact axons which are exposed to extremely high levels of nerve growth factor (NGF) and glial cell line-derived neurothrophic factor (GDNF), leading to hyperexcitability and sprouting. NGF causes immediate excitability of nociceptors in the afferents. Moreover, retrograde transport of NGF to the neuronal cell body causes up-regulation of pro-excitatory proteins, including the transient receptor potential cation channel subfamily V member 1 (TRPV1) and down-regulation of anti-excitatory proteins, such as voltage-activated potassium channels; Fig 19B. Dynamic denervation neuropathies are caused by inflammatory processes. Pro-inflammatory cytokines may induce direct activation of regrowing or retracting nociceptors, enhancing pain signalling. This in combination with an overstimulating environment for the intact nociceptors, results in hypersensitivity. PDN and HIV-associated neuropathy are examples of a disease with a dynamic denervation; Fig 19C. Static and dynamic denervation neuropathies are characterized by a decrease in nerve fibre density; however some chronic pain syndromes have an overall increased nociceptor density. Vulvodynia [68] and burning mouth syndrome [69] are such conditions. Denervation in these conditions may be followed by abundant re-innervation, called hyperinnervation; Fig 19D.
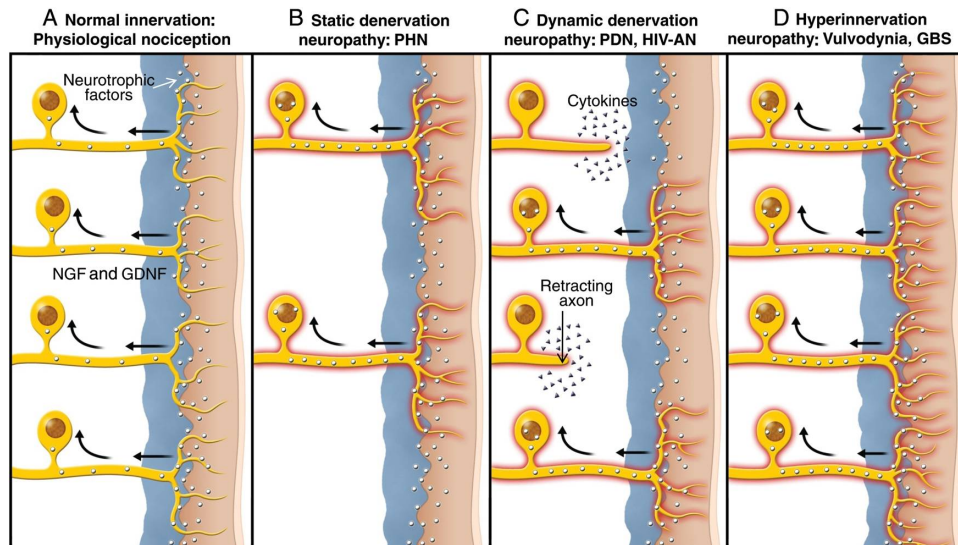
Figure 19: Different forms of skin innervation may be used to classify neuropathic pain syndromes with different etiologies. Adapted from Anand and Bley [67]
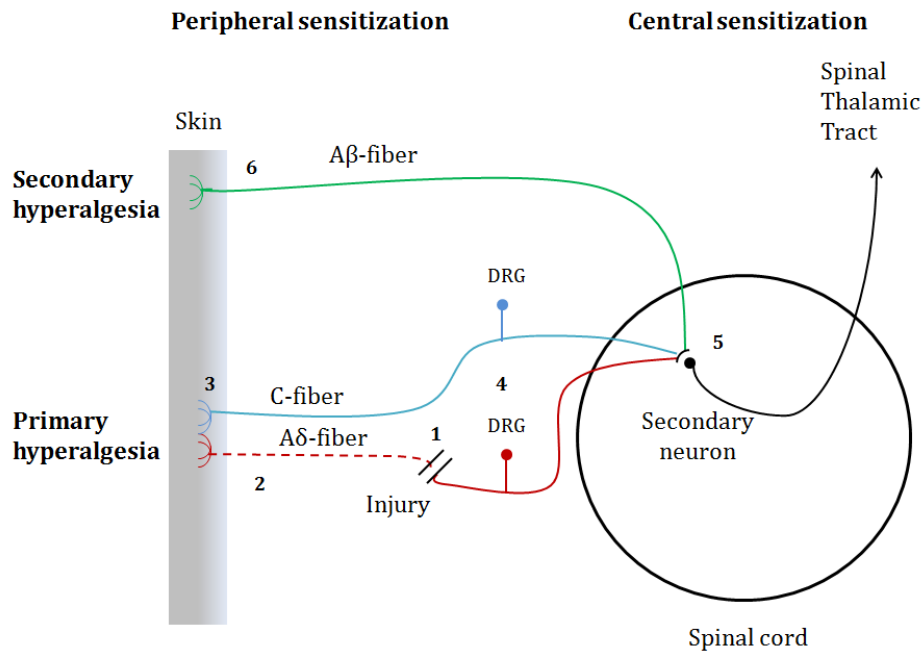

Figure 20: Pathophysiological changes after a nerve injury in a neuropathic pain patient. 1) At the site of the nerve injury, spontaneous nociceptive activity develops 2) The distal part of the injured axon undergoes Wallerian degeneration, resulting in an increase of cytokines, NGF and other algesic factors 3) Hypertrophic environment overstimulates uninjured nerve fibres, causing peripheral sensitization 4) Up- and down-regulation of proteins in the DRG promote nociceptive input 5) Windup may cause central sensitization 6) Surrounding healthy tissue gets sensitized for mechanical stimulation.

Nerve injury and long lasting overstimulative sprouting could have a high impact on the pain perception. When a nerve fibre axon is interrupted by a traumatic, toxic, ischaemic or surgical event, the injury triggers a cascade of alterations influencing the nociception, see Fig 20. At first, the injured nerve forms into a non-neoplastic neuroma with an increased sodium channel expression and spontaneous activity [70]. The distal part of the injured axon undergoes Wallerian degeneration. This results in the release of cytokines, NGF and other algesic factors in the peripheral tissue, dependent on the innervation type

(see Fig 19). The hyperexcitability of the neuroma and of the same innervated uninjured nerves cause up- and down-regulation of several proteins in the dorsal root ganglions (DRGs) promoting neuronal activity [71, 72]. Accumulation of nociceptive activity sensitizes the secondary neuron in the spinal cord by the 'wind-up effect' and is important for central sensitization. As a consequence of central sensitization non-painful mechanical stimuli in the surrounding healthy tissue may be experienced as painful.

Neuropathic pain reflects both peripheral and central sensitization mechanisms. Baron et al. [73] suggested a new mechanism based classification of neuropathic pain combined with a selection of drugs that act on those mechanisms to optimize the treatment for individuals. For this taxonomy, not the disease state of the patient, but the phenotypic characterization of the neuropathic pain is important. To simulate phenotypic characteristics of a neuropathic pain syndrome in healthy subjects, human experimental pain models can be used.

Appendix II: Psychophysical data analysis

In a psychophysical experiment, an extended range of stimuli may be presented in which the subject indicates which stimulus is observed. The probability of an observed stimulus is in turn dependent on the intensity of the stimulus, the guess rate and lapse rate. This relationship can be modeled by a psychometric function to extract relevant parameters that summarize the stimulus-response interaction. The generic formulation of the psychometric function according to Kingdom et al. [11] is:

$$\psi(x, \gamma, \lambda) = \gamma + (1 - \gamma - \lambda)F(x) \tag{4}$$

with ψ = probability, x = stimulus intensity, α = detection threshold, β = slope, λ = lapse rate.

In Equation 4 (Fig 21), the guess rate (γ) is the probability of a correct response when the stimulus is not detected by the underlying sensory mechanism and the lapse rate (λ) is the probability of an incorrect response which is independent of the stimulus intensity. The more interesting function is $F(x)$, which describes the probability of detection of the stimulus by the underlying sensory mechanism as a function of stimulus intensity x. Commonly used $F(x)$ functions are logistic, Weibull, cumulative normal distribution, Gumbel or hyperbolic secant function [11]. The reason for choosing a particular function is dependent on different mathematical assumptions. For instance, the cumulative normal distribution and the logistic function are inappropriate to use when a stimulus intensity $x = 0$ corresponds to the absence of a signal, unless x is log-transformed. This is because $F_N(x = 0) > 0$ and $F_N(x) = 0$ for $x \to \infty$ for all values.

Nevertheless, each type shows a sigmoidal form which can be broken down into two useful parameters. The first parameter, usually called the threshold (α), determines the overall position of the curve along the abscissa. For a logistic function, this corresponds to the stimulus intensity at which the probability is halfway between the lower and upper asymptote. In Figure 12 this resembles 0.75 or 75% correct, but could also be 0.5 or 50% correct. The second parameter determines the slope or gradient of the curve (β) and gives information on the discriminative ability of the subject.
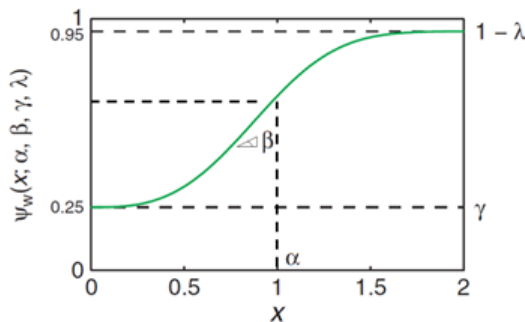

Figure 21: Generic formulation of the psychometric function. The probability ψ is in this case modeled by the Weibull function $F(x; \alpha, \beta)$. Illustration adapted from Kingdom et al.[11], x= stimulus intensity, α = threshold

Estimation of these parameters in an psychophysical experiment is dependent on a stimulus selection procedure and a method to fit the experimental data of stimulus-response pairs to the pre-defined psychophysical function [74]. Since the method of IES is restricted to stimulate at maximal twice the detection threshold, experiments are needed to estimate this threshold beforehand. Relationships between stimuli and responses in a detection experiment can be modeled by a sigmoidal curve. This sigmoidal form may be described by a logistic link function encompassing both the threshold α and the slope β (Eq 5). The threshold in IES experiments is often defined as the stimulus amplitude that represents the detection probability of 0.5, or 50%. The slope β describes the steepness of the curve and can be used as a measure of internal background noise, i.e. how easily the stimulus can be detected (Fig 1). Since these parameters are sensitive to change in human experimental pain models [12, 13, 14, 15, 75], they are used as parameters in quantification of nociception.

$$p(x; \alpha(t), \beta) = \left(1 + e^{\beta(\alpha(t)-x)}\right)^{-1} \qquad (5)$$

with p = detection probability, x = stimulus intensity, $\alpha(t)$ = detection threshold over time, β = slope

To estimate these parameters, the psychophysical curve must be probed by varying stimulus amplitudes and measured by detected and non-detected responses. The method to do this is called the stimulus selection procedure. Stimulus selection procedures can be either adaptive or non-adaptive. Non-adaptive procedures don't take into account information of past stimuli and responses. Therefore, predefined stimuli over time are required before the start of an experiment to probe the psychophysical curve. These kind of procedures are relatively inefficient for accurate estimation of threshold and slope [76]. Therefore, adaptive procedures have been developed that use information of the previous stimulus and response pairs. A simple and common adaptive procedure is the up-down staircase procedure [77]. This procedure increases the stimulus with a designated step size after a non-detected response and vice versa. Therefore, the stimulus selection will end up converging around the detection threshold. Although this is a simple and efficient procedure, it enables anticipation of the subject and loses information about the slope. For these reasons, Doll et al. introduced a new method that combined unpredictability in an adaptive stimulus procedure, called the random staircase procedure [74]. Stimuli are randomly selected from a small predefined set of amplitudes, but this set also moves up and down according to the staircase procedure. This advanced procedure combines best of both worlds and is used in this study. The next Appendix elaborates on the stimulus selection procedure for this study.

Appendix III: Stimulus selection procedure

Intra-epidermal electrical stimulation (IES) has been developed to stimulate Aδ fibers preferentially. However, the stimulus current should be below twice the detection threshold to limit co-activation of Aβ fibers. Since the detection threshold varies inter- and intra-individually, this should be estimated experimentally before evoked potentials (EPs) in the EEG can be analyzed reliably. Therefore, the experiment is divided into two parts. The goal of Part I is to use a stimulus selection procedure method that retrieves the detection thresholds and slopes of both single pulse and double pulse stimuli with reasonable quality in the least amount of time. The goal of Part II is stimulating at 1.5x and 2x the detection threshold of both single pulse and double pulse stimuli to retrieve reliable EPs (Fig 22).

Stimulus selection procedures can be either adaptive or non-adaptive. Non-adaptive procedures don't take into account information of past stimuli and responses. Therefore, predefined stimuli over time are required before the start of an experiment to probe the psychophysical curve. These kind of procedures are relatively inefficient for accurate estimation of threshold and slope [76]. Therefore, adaptive procedures have been developed that use information of the previous stimulus and response pairs. A simple and common adaptive procedure is the up-down staircase procedure [77]. This procedure increases the stimulus with a designated step size after a non-detected response and vice versa. Therefore, the stimulus selection will end up converging around the detection threshold. Although this is a simple and efficient procedure, it enables anticipation of the subject and loses information about the slope. For these reasons, Doll et al. introduced a new method that combined unpredictability in an adaptive stimulus procedure, called the random staircase procedure [74]. Stimuli are randomly selected from a small predefined set of amplitudes, but this set also moves up and down according to the staircase procedure. This advanced procedure combines best of both worlds and therefore is used in this study.
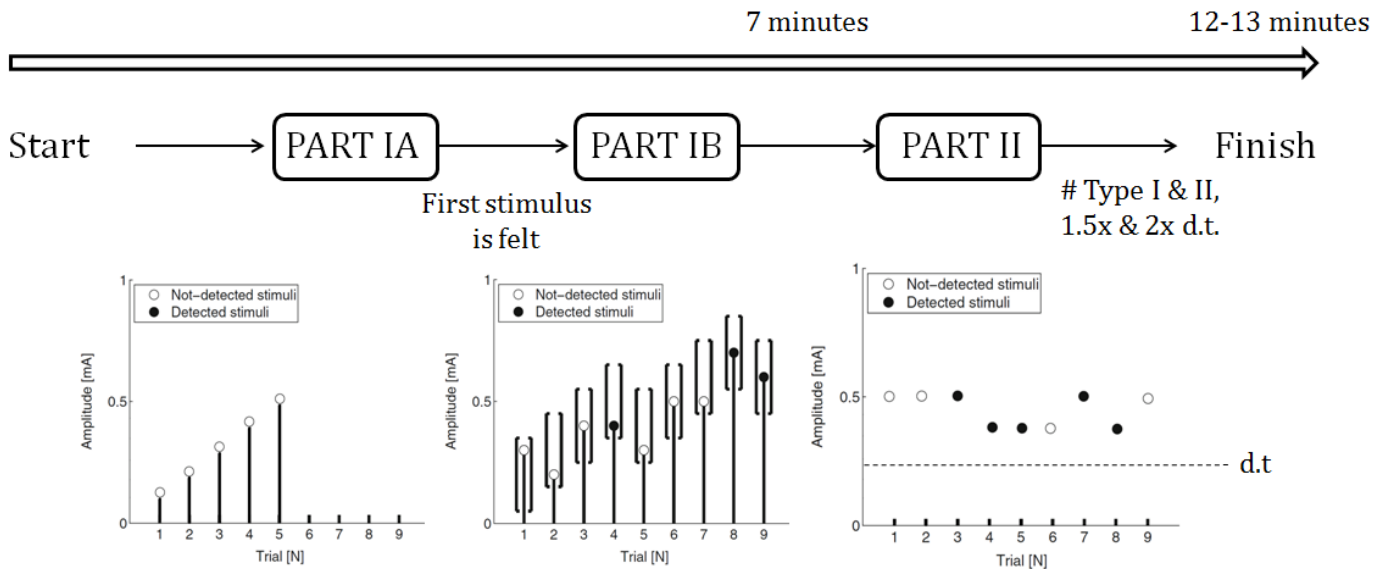

Figure 22: Timeline of stimulus selection procedure. Part Ia consists of a simple staircase (steps of 0.1 mA) until the first stimulus is felt. Part Ib consists of a random staircase procedure with a probability vector moving up and down. Part II consists of 80 stimulations, of which 20 stimulations per type per amplitude (1.5x and 2x detection threshold).

For the random staircase procedure (Part Ib) two parameters should be chosen: the number of stimulus amplitudes in the probability vector and the step size between these amplitudes (Fig 23). These parameters were optimized for the bias and variance of the detection threshold and slope using Monte Carlo simulations.
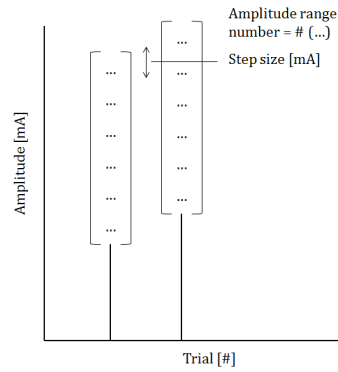
Figure 23: Input parameters for choosing the optimal stimulus selection procedure were the amplitude range number and step size.

Twelve situations were considered in which the true threshold and true slope were varied. The input for the simulations were different step sizes and amplitude range numbers. The output for the simulations were the bias and variance in threshold, slope and error in the amplitude. For each input parameter and situation 100.000 experiments were simulated using a random generator in the random staircase procedure. Since 16 input parameters and 12 situations were evaluated, a total of 16x12x100,000 = $19.2 \cdot 10^6$ simulations were run.
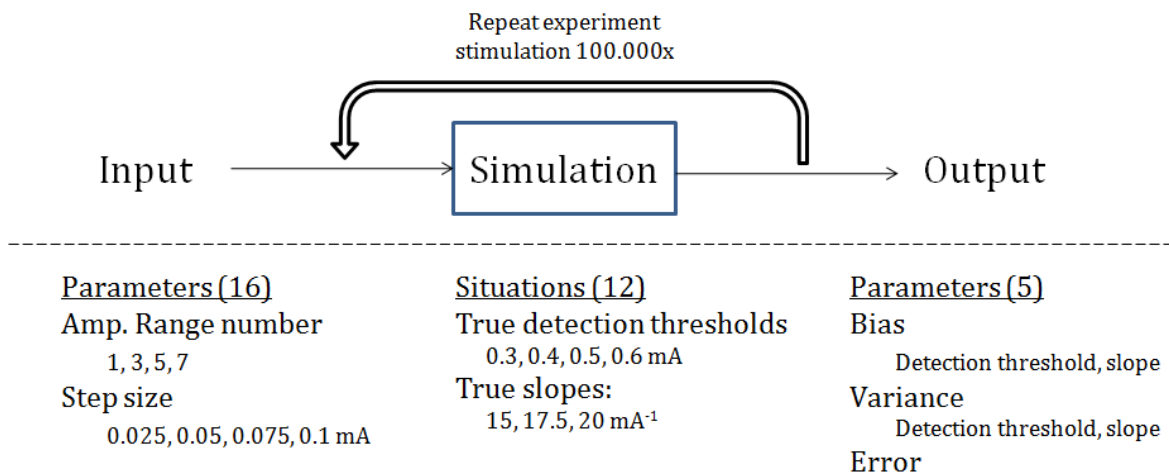

Figure 24: Overview of Monte Carlo simulations for optimizing the stimulus selection parameters.
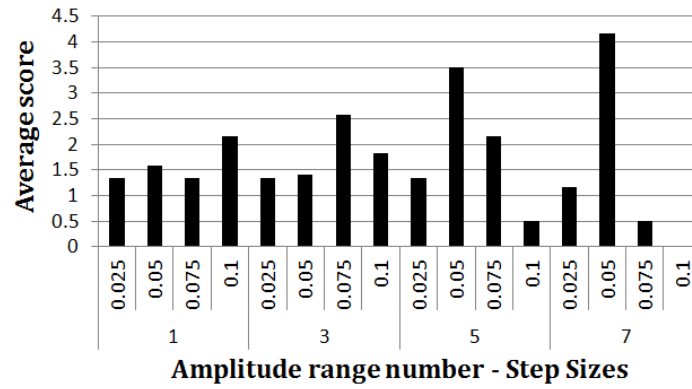
Figure 25: Result of overall scores for all stimulus selection parameters averaged over 12 situations.

The analysis of the output parameters was done by scoring the top 20% results with a 1 and the the bottom 80% results with a 0 for all input parameters in each situation. Subsequently, the input parameters were averaged for all 12 situations. The results are shown in Fig 25. As can be seen, the amplitude range number of 7 with a step size of 0.05 mA scored highest and this combination was therefore chosen as the stimulus selection parameters.
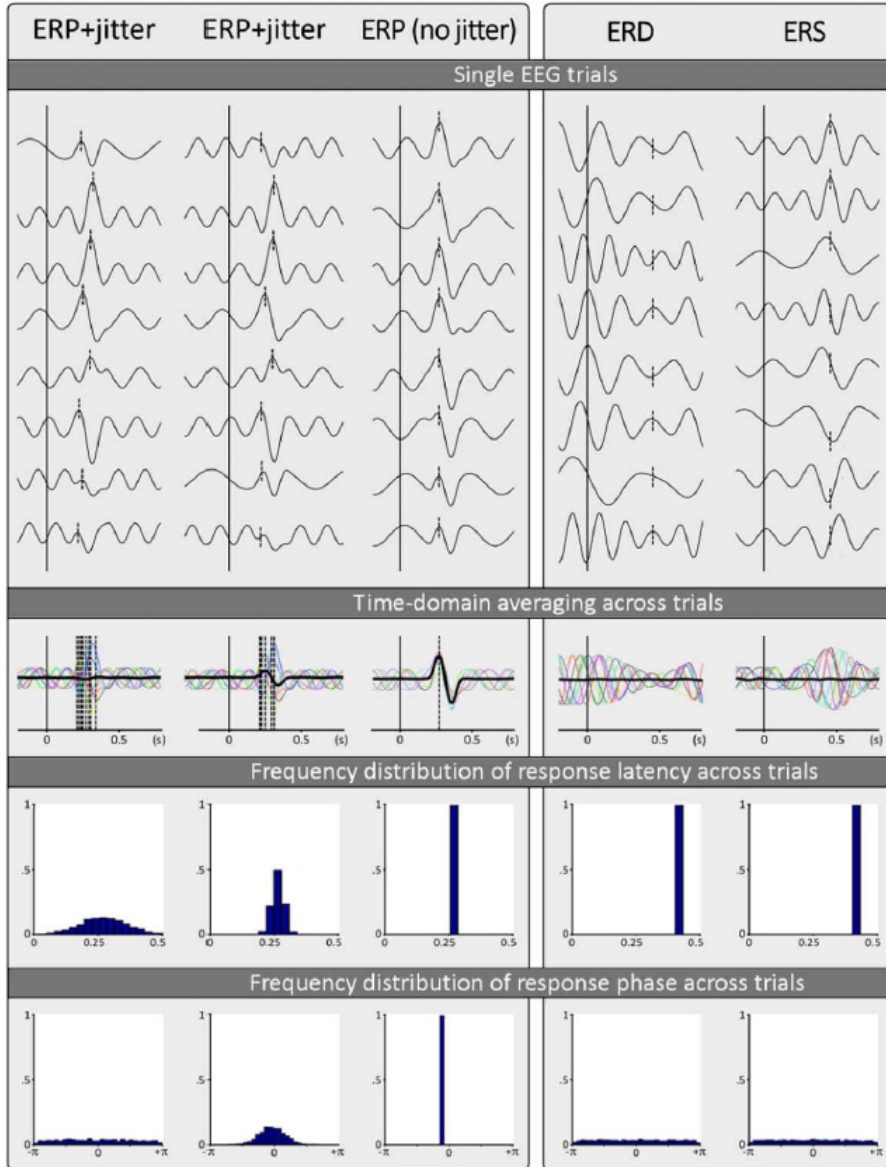
Appendix IV: Non-phase locked analyses

Figure 26: Effect of time-averaging of EEG evoked responses on information loss. When single EEG trials show time-locked and non-phase locked properties, time-domain averaging may lose information. In the left panel (ERP), the latency of the response was either varied from trial to trial using a significant jitter (left waveforms) or a moderate jitter (middle waveforms), or constant across trials (right waveforms). In the right panel (ERD and ERS), ERD and ERS were modeled as time-locked decreases or increases of the amplitude of ongoing, non-phase-locked oscillations. Illustration from Mouraux et al. [27]

Non-phase locked EP information may be lost due to time-averaging (Fig 26). When the cortical activity is temporally dispersed, the electrical response will be diluted over time, i.e. latency jitter. This may be caused by variable conduction velocities (especially for C-fibers) or variable transduction processes, e.g. thermal to electrical energy for laser stimulation. A solution for this specific problem is analyzing non-phase locked data as well. The existing methods are based on estimating the amplitude of oscillations as a function of time and frequency within each single EEG trial. Since this analysis is phase independent, averaging across trials shows both phase locked and non-phase locked effects.

Assessment (Time point)	SCR — Up to -28 d	Pre-dose	-30MIN	0HR	20MIN	1HR	3HR	5HR	8HR	10HR	Follow up[1] +14 d ± 2 d
		Study Period 1 & 2 (Optional 3rd)									
Screening assessments[2]	X										
Vital signs (BP, HR, temperature)	X	X									
UrDrug, BrAlc	X	X									
General symptoms	X	X									X
Conmed	X	X									X
Capsaicin application	X[4]		X								
Remove capsaicin	X[4]										
Pre-/Rekindling[3,4]	X[4]		X	X							
Multispectral imaging		X			X		X	X	X		
Laser speckle imaging		X			X	X	X	X	X	X	
Capsaicin task – Von Frey test					X	X	X	X	X	X	
Capsaicin task - IES	X[4]	X				X	X	X	X		
Capsaicin task – LS	X	X				X	X	X	X		
Capsaicin task – LS - NRS	X[5]	X				X	X	X	X		
Capsaicin task - Thermal stimulation					X	X	X	X	X	X	
Capsaicin - NRS[6]	X				X	X	X	X	X	X	
McGill Pain Questionnaire[7]							X				
Meals / snack			X						X	X	
Discharge	X									X	
(S)AE/Con-meds					<----- continuous ----->						

SCR = Screening, BP = Blood Pressure, HR = Heart Rate, UrDrug = Urine Drug, BrAlc = Breath Alcohol Test, IES = intra-epidermal electrical stimulation, LS = laser stimulation, EEG = Electro-encephalogram, AE = adverse event.

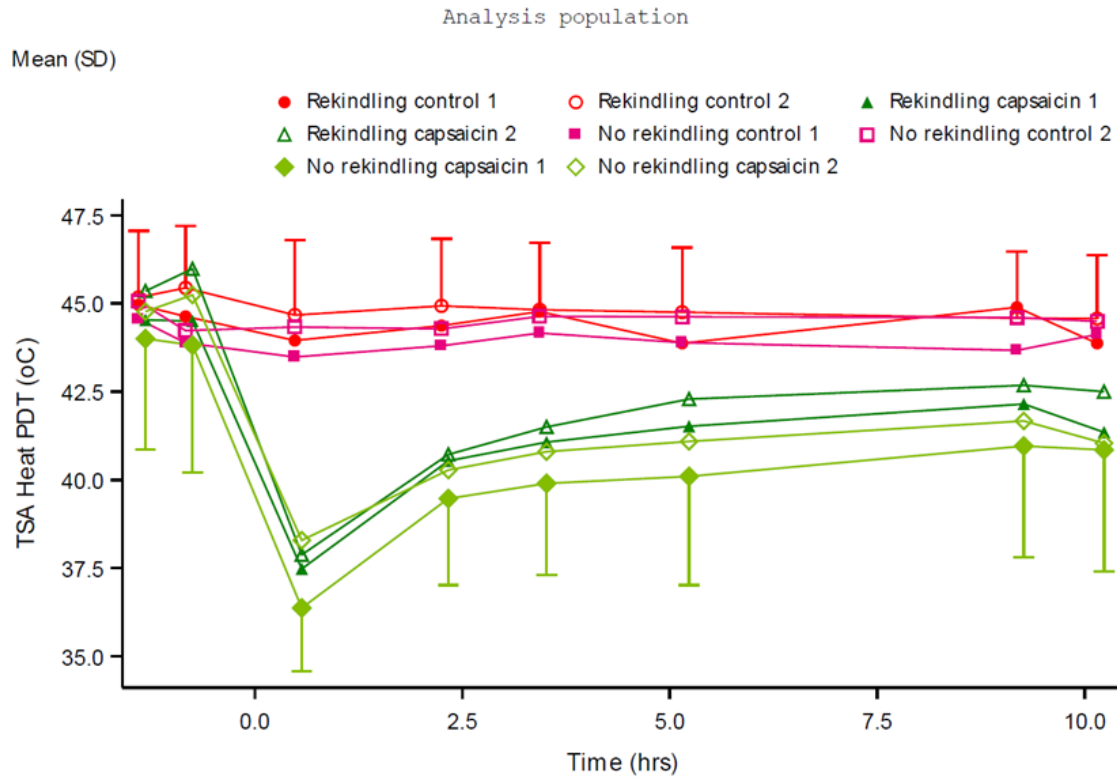# Appendix VI: Results primary heat hyperalgesia

Figure 27: Effect of capsaicin on heat pain detection thresholds. Capsaicin affected area shows clear significant reductions after the double baseline measurement, while control area remains at the same level. This supports the fact that capsaicin induced heat hyperalgesia. In addition, rekindling (reheating of the skin) did not have any significant effect on the heat pain detection threshold. PDT = pain detection threshold, TSA = thermode analyzer.

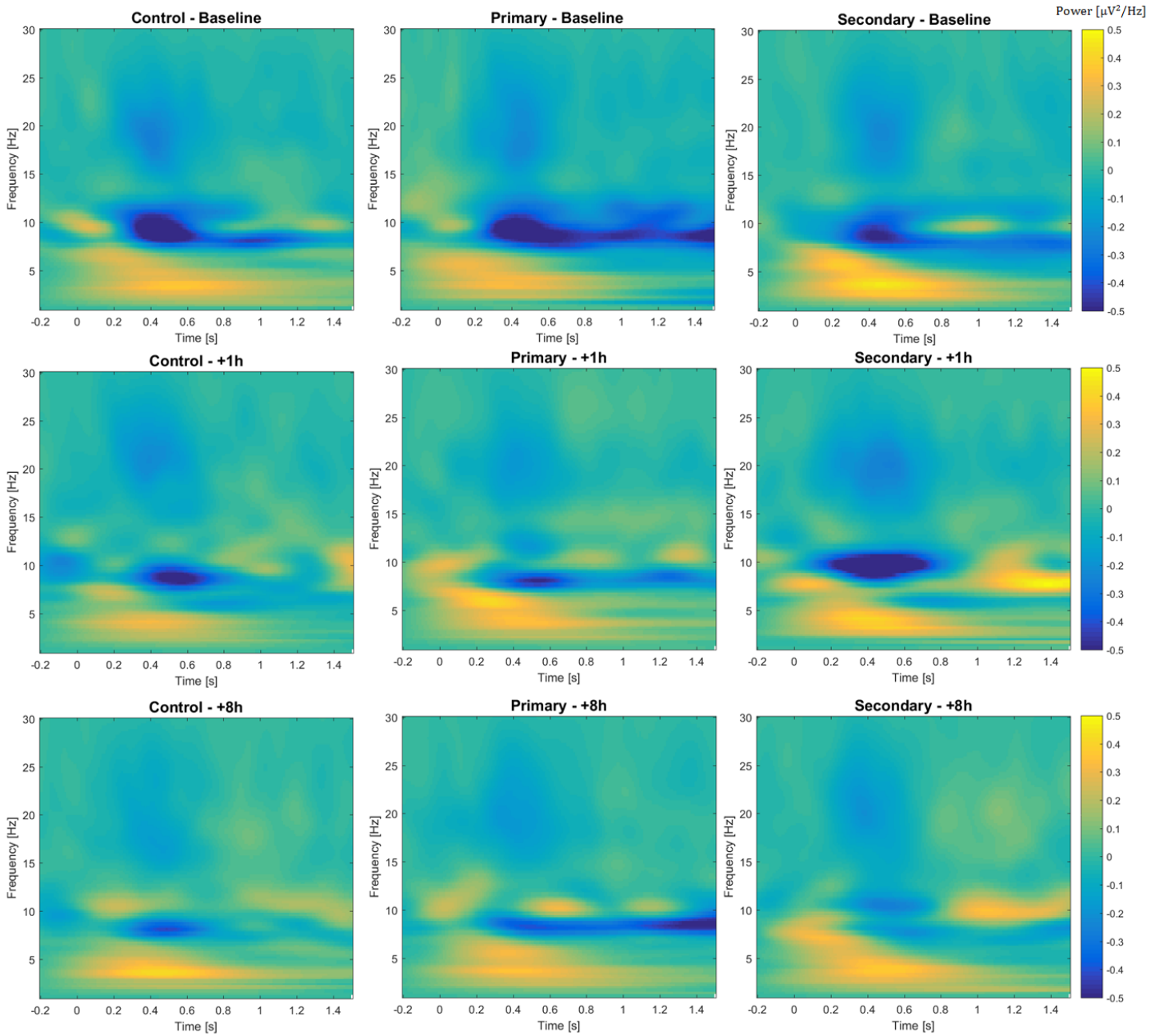# Appendix VII: Time-frequency representations - Grand averages

Figure 28: Grand averages of time-frequency representations per area per measurement.

Appendix VIII: Standard Operating Protocols

All operations were performed at the Centre for Human Drug Research (CHDR), which is a contract research organisation that focuses on phase I drug development. For each pharmacodynamic assessment, standard operating protocols (SOPs) were created. A selection of the SOPs that were related to this paper are attached at the end of this document.